AIMS Biophysics

AIMS Biophysics, 11(2): 189–233.
DOI: 10.3934/biophy.2024012
Received: 06 March 2024
Revised: 26 April 2024
Accepted: 27 May 2024
Published: 04 June 2024

http://www.aimspress.com/journal/biophysics

Research article

A mathematical modeling of the mitochondrial proton leak via quantum tunneling

Mahmoud Abdallat[1], Abdallah Barjas Qaswal[2,*], Majed Eftaiha[3], Abdel Rahman Qamar[4], Qusai Alnajjar[5] ,Rawand Sallam[5], Lara Kollab[5], Mohammad Masa'deh[5],Anas Amayreh[6], Hiba Mihyar[7], Hesham Aboushakra[8], Bayan Alkelani[8], Rawan Owaimer[8], Mohannad Abd-Alhadi[9], Salwa Ireiqat[10], Fahed Turk[11], Ahmad Daoud[12], Bashar Darawsheh[13], Ahmad Hiasat[14], Majd Alhalaki[15], Shahem Abdallat[16], Salsabiela Bani Hamad[17] and Rand Murshidi[17]

[1] Department of Neurosurgery, Jordan University Hospital, School of Medicine, University of Jordan, Amman 11942, Jordan
[2] Department of Psychiatry, Jordan University Hospital, Amman 11942, Jordan (A.B.Q)
[3] Department of Neurosurgery, Jordan University Hospital, Amman 11942, Jordan
[4] School of Medicine, The Hashemite University, Zarqa 13133, Jordan. (A.R.Q)
[5] Department of Internal Medicine, Jordan University Hospital, Amman 11942, Jordan
[6] Department of General Surgery, Jordan University Hospital, Amman 11942, Jordan
[7] Department of Emergency, Jordan University Hospital, Amman 11942, Jordan
[8] Department of Family Medicine, Jordan University Hospital, Amman 11942, Jordan
[9] School of Medicine, Near East University, Nicosia, Cyprus
[10] School of Medicine, Jordan University of Science and Technology, Irbid 22110, Jordan
[11] Tver State Medical University, Ulitsa Sovetskaya, 4, Tver, Tver Oblast, Russia, 170100
[12] Cardiovascular Research Department, King's College London, London WC2R 2LS, United Kingdom
[13] School of Medicine, Yarmouk University, Irbid 21163, Jordan
[14] Hamad Medical Corporation, PO Box 3050 Doha, Qatar
[15] School of Medicine, University of Jordan, Amman 11942, Jordan
[16] School of Medicine, Xavier University, Santa Helenastraat 23, Oranjestad, Aruba
[17] Department of Dermatology, Jordan University Hospital, Amman 11942, Jordan

* **Correspondence:** Email: qaswalabdullah@gmail.com.

Abstract: The mitochondrion is a vital intracellular organelle that is responsible for ATP production.

It utilizes both the concentration gradient and the electrical potential of the inner mitochondrial membrane to drive the flow of protons from the intermembrane space to the matrix to generate ATP via ATP-synthase. However, the proton leak flow, which is mediated via the inner mitochondrial membrane and uncoupling proteins, can reduce the efficiency of ATP production. Protons can exhibit a quantum behavior within biological systems. However, the investigation of the quantum behavior of protons within the mitochondria is lacking particularly in the contribution to the proton leak. In the present study, we proposed a mathematical model of protons tunneling through the inner mitochondrial membrane and the mitochondrial carrier superfamily MCF including uncoupling proteins UCPs and the adenine nucleotide translocases ANTs. According to the model and its assumptions, the quantum tunneling of protons may contribute significantly to the proton leak if it is compared with the classical flow of protons. The quantum tunneling proton leak may depolarize the membrane potential, hence it may contribute to the physiological regulation of ATP synthesis and reactive oxygen species ROS production. In addition to that, the mathematical model of proton tunneling suggested that the proton-tunneling leak may depolarize the membrane potential to values beyond the physiological needs which in turn can harm the mitochondria and the cells. Moreover, we argued that the quantum proton leak might be more energetically favorable if it is compared with the classical proton leak. This may give the advantage for quantum tunneling of protons to occur since less energy is required to contribute significantly to the proton leak compared with the classical proton flow.

Keywords: quantum tunneling; quantum biology; mitochondria; proton leak; UCPs; ANTs

Abbreviations: Adenosine triphosphate: ATP; Proton motive force: pmf; Adenine nucleotide translocase: ANT; Uncoupling protein: UCP; Reactive oxygen species: ROS; Adenosine diphosphate: ADT; Guanosine triphosphate: GTP; Guanosine diphosphate: GDP; Mitochondrial carrier superfamily: MCF; Inner mitochondrial membrane: IMM; Potential mean force: PMF; Intermembrane space: IMS; Electron transport chain: ETC

1. Introduction

The mitochondrion is a vital cellular organelle that produces energy in the form of adenosine triphosphate ATP [1,2]. In addition, mitochondria are involved in several important cellular functions, which include carbon and nitrogen metabolism, oxidation of sugars, fats, and proteins, ion hemostasis, and programmed cell death mediated via caspases [1,2]. The energy production is based on maintaining the proton gradient across the inner mitochondrial membrane and the flow of protons from the intermediate space to the matrix through the ATP synthase is responsible for ATP synthesis [1,2]. According to Mitchell's chemiosmosis hypothesis, pumping protons against their concentration gradient from the matrix to the intermembrane space creates a proton motive force (pmf). This pmf drives the flow of protons from the intermembrane space back to the matrix going through the enzyme ATPase that catalyzes the production of ATP [1,2]. The pmf is generated due to the concentration difference across the inner mitochondrial membrane and its electrical potential which is negative at the matrix side relative to the intermembrane space [1,2]. However, protons can flow across mediators other than the ATP synthase and this flow is called proton leak. A proton leak across the membrane can affect the chemical proton gradient, the electrical potential of the inner membrane, and thus the motive

force for proton flow [3−8]. Thus, the proton leak can affect the efficiency of ATP synthesis. It behaves in a non-ohmic pattern, which means the relationship between the proton current and the voltage is not linear but rather exponential [8]. There are two types of proton leak: 1) The basal proton leak and 2) the inducible proton leak. The basal proton leak is mediated via the lipid bilayer of the inner mitochondrial membrane, the adenine nucleotide translocases (ANTs), and uncoupling proteins (UCPs). However, the proton leak is not mediated via the protein activity of these carriers because it was shown that the proton leak was produced even though inhibitors for these carriers were added [8]. On the other hand, the inducible proton leak requires the activation of mitochondrial anion carrier protein function and is catalyzed by ANTs and UCPs [8]. The physiological function of the proton leak is to uncouple between oxidation and phosphorylation to protect against excessive reactive oxygen species ROS production [8]. The inducible proton leak is activated by free fatty acids and superoxide ions, while it is inhibited by purine nucleoside di- and tri-phosphates including ADP, ATP, GDP, and GTP. The proton leak reduces ROS production by decreasing the rate of ATP production via two mechanisms: 1) It uncouples the oxidation from phosphorylation by bypassing the flow through the ATP-synthase [8]. 2) The proton leak can depolarize the electrical potential of the inner mitochondrial membrane IMM, hence it will reduce the electrical gradient that is necessary to drive the protons through the ATP synthase [9–11]. Therefore, fine regulation of the electrical potential of the inner mitochondrial membrane IMM is crucial to provide sufficient ATP for cellular functioning and decrease the amount of reactive oxygen species ROS produced. The ANTs and UCPs are considered members of the mitochondrial carrier superfamily (MCF) proteins. These proteins have a common molecular structure in which they contain two salt-bridge networks, which are at the cytoplasmic and matrix sides. Breaking down the salt bridges of these networks results in the proton flow through the MCF proteins. These cytoplasmic and matrix networks serve as gates that control the flow of protons [8]. During the flow of protons, the MCF protein alternates between the cytoplasmic and matrix states to allow the passage of protons [8].

A Proton is a particle that can show quantum mechanical behavior and obey the mathematical formalism of quantum mechanics including the Schrödinger equation. According to quantum mechanics, the proton has a wave-particle duality which means that it can behave like a particle and a wave. Its wave behavior is studied using the principles of quantum mechanics [12]. For this reason, researchers have theoretically and experimentally started studying the quantum wave behavior of protons and other particles within biological systems in the so-called field of quantum biology [13,14]. Biologists have been thinking about the role of the quantum mechanical phenomena, including tunneling in cellular functions and the mitochondrial electron transport chain, and the process of electron bifurcation [13,14]. Interestingly, the proton received considerable attention by quantum biologists to investigate its quantum wave behavior within biological systems [15,16]. This implies that the quantum wave behavior can contribute to the biological actions and processes. They have applied the phenomenon of quantum tunneling on protons to explain the enzymatic reactions and the point mutations of DNA [17–19]. The mitochondrion is a promising molecular target to utilize the quantum mechanical formulation to explore the quantum mechanical aspects of the biological and cellular functions [15]. Researchers have focused on electrons as candidate quantum particles to investigate the quantum mechanical aspects of the physiological functions of mitochondria [20−23]. However, protons, which are crucial for ATP production, did not receive enough attention in the context of their quantum mechanical behavior.

In this study, we aim to show that the quantum tunneling of protons through the IMM and its

proteins can serve as a proton leak that can control ATP and ROS production and may be implicated in the pathogenesis of several neurodegenerative diseases. In the present work, we explored the role of the quantum behavior of protons particularly quantum tunneling in the proton leak flow through the inner mitochondrial membrane. See Scheme 1.

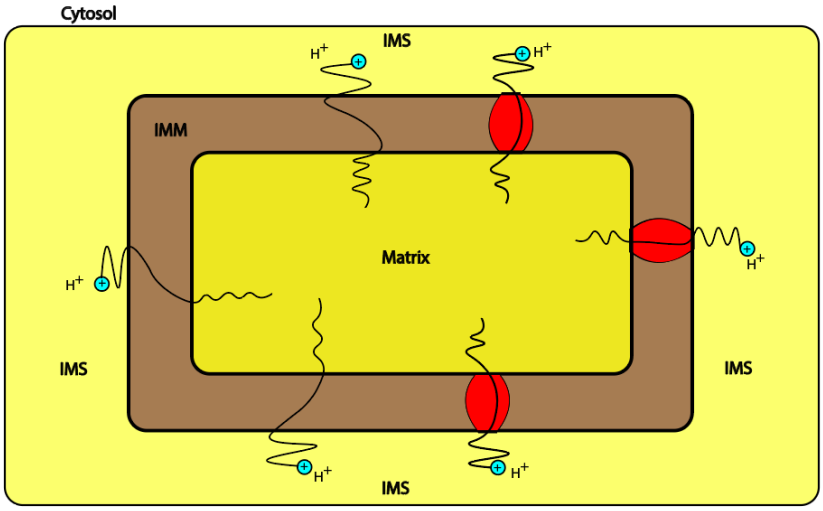

Scheme 1. A schematic diagram of the proton tunneling through the inner mitochondrial membrane IMM and the MCF proteins (shown in red). The scheme illustrates the net quantum tunneling of protons to the matrix of mitochondria serving as a leak current to control the production of ATP and ROS.

2. The mathematical model

A mathematical model of quantum tunneling of ions has been proposed and applied to the voltage-gated channels showing several pathophysiological and clinical implications [24,25]. In the present study, the model of quantum tunneling will be applied to protons while passing through the inner mitochondrial membrane IMM and MCF proteins. In this model, protons are treated as quantum waves that can tunnel through the closed gates of the MCF proteins. The barrier height of these gates is larger than the kinetic energy of protons and thus they are classically impermeable. The molecular structure of the MCF indicates that the proton flow is impeded at the two ends of the inner mitochondrial membrane; the matrix and cytoplasmic ends [8]. Hence, two energy barriers can control the flow of protons through these proteins. Moreover, the inner membrane itself limits the flow of protons due to its hydrophobic nature. Accordingly, the proton tunneling can be applied to MCF proteins and the lipid bilayer of IMM.

There are several shapes of the barrier through which quantum tunneling occurs. The barrier shape of the hydrophobic materials as in the case of IMM can be mimicked using the triangular shapes as obtained using the potential mean forces (PMFs) [26−28]. See Figure 1. The barrier shape of the salt-bridge networks has not been studied using the potential mean forces. Hence, we will use the same triangular shapes of the IMM for the salt-bridge networks, which are reasonable shapes used frequently in biological simulations.

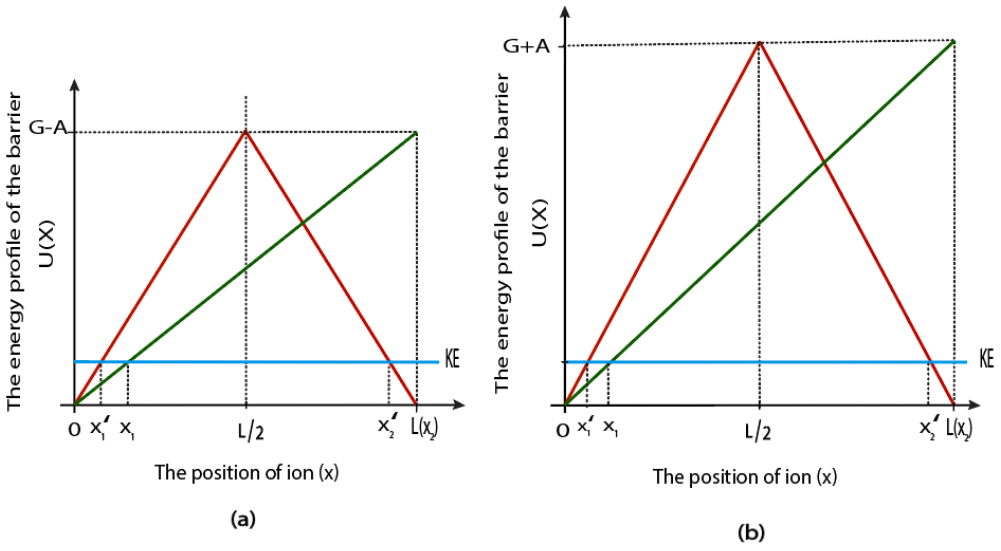

Figure 1. The figure represents the energy profile of the barriers that block the permeation of protons. The shape of the energy barrier takes the shape of the triangle that is illustrated by the red and the green graphs that are equivalent in terms of the tunneling probability of protons as will be shown below. The blue line represents the kinetic energy of the proton. Factor A represents a factor that can increase or decrease the barrier height, which will be explained later.

Based on Figure 1, the triangular shape of the barrier can take two forms, which are the right angle triangle (green in color) and the isosceles triangle (red in color). The right angle triangle indicates that the potential energy of the barrier increases linearly as the ion passes through the barrier until reaching the highest point of energy at the end of the barrier. On the other hand, the isosceles triangle indicates that the potential energy of the barrier increases linearly until reaching the highest point of energy at the middle of the barrier and then starts to decrease until the end of the barrier.

A possible mechanism of sealing off the permeation of ions including protons is dewetting/dehydrating the pore [27]. As the number of water molecules in the pore decreases, the barrier height will increase and the flow of ions will diminish and vice versa [27]. Moreover, a recent investigation found that the electrical field increases the hydration of the pore and increases the conduction of ions [29].

The energy profile of the green graph can be mathematically represented by the following equation:

$$U(x) = (\frac{G}{L} \mp \frac{a}{L_a})x, 0 \geq x \geq L, \quad (1)$$

where G is the original barrier height, L is the length of the barrier, $\frac{a}{L_a}$ is a factor related to the factor A which decreases or increases the original barrier height G. In this term $A = \frac{a}{L_a}$; $a = q_{H^+} V_m$ in which q_{H^+} is the charge of proton, V_m is the electrical potential of IMM and L_a represents the length of the inner mitochondrial membrane L_{IMM}. These variables and their relations to each other will be

explained later.

On the other hand, the energy profile of the red graph can be mathematically represented by the following equation:

$$U(x)=\begin{cases}2(\frac{G}{L}\mp\frac{a}{L_a})x, 0\geq x\geq\frac{L}{2}\\ -2(\frac{G}{L}\mp\frac{a}{L_a})(x-L), \frac{L}{2}\geq x\geq L\end{cases}, \quad (2)$$

The tunneling probability of protons through these biological barriers can be estimated using the 1-D Wentzel–Kramers–Brillouin (WKB) approximation [12,30]:

$$T=e^{\frac{-\sqrt{8m}}{\hbar}\int_{x1}^{x2}\sqrt{U(x)-KE}dx}, \quad (3)$$

where m is the mass of proton and $\hbar$ is the reduced Planck constant.

Concerning the MCF proteins, there are two energy barriers. Therefore, the protons should tunnel through both of them to complete their passage to the other side of the inner mitochondrial membrane. See Figure 1.

Both triangular shapes are equivalent in terms of tunneling probability that can be calculated by the following equation:

$$T=\frac{2}{3(\frac{G}{L}\mp\frac{a}{L_a})}\sqrt{(\mathrm{G}\mp\frac{aL}{L_a}-KE)^3}, \quad (4)$$

See the appendix at the end of the article for the mathematical derivation of Eq (4).

2.1. The quantum tunneling of protons through the inner mitochondrial membrane IMM

The protons at both sides of the IMM have the opportunity to tunnel through it. Since the electrical potential of the IMM is positive at the IMS side, it is expected that the tunneling of the IMS protons to the matrix has a higher probability compared to the tunneling probability in the opposite direction of the matrix protons. See Figure 2.

2.1.1. The quantum tunneling of intermembrane space IMS protons

The IMS protons will encounter the energy barrier of the lipid bilayer of IMM. However, the electric field across the IMM will reduce the barrier height for IMS passage from the IMS side to the matrix side because their direction of flow is the same as the electric field. In addition, their kinetic energy will be attained from the thermal biological environment. See Figure 2.

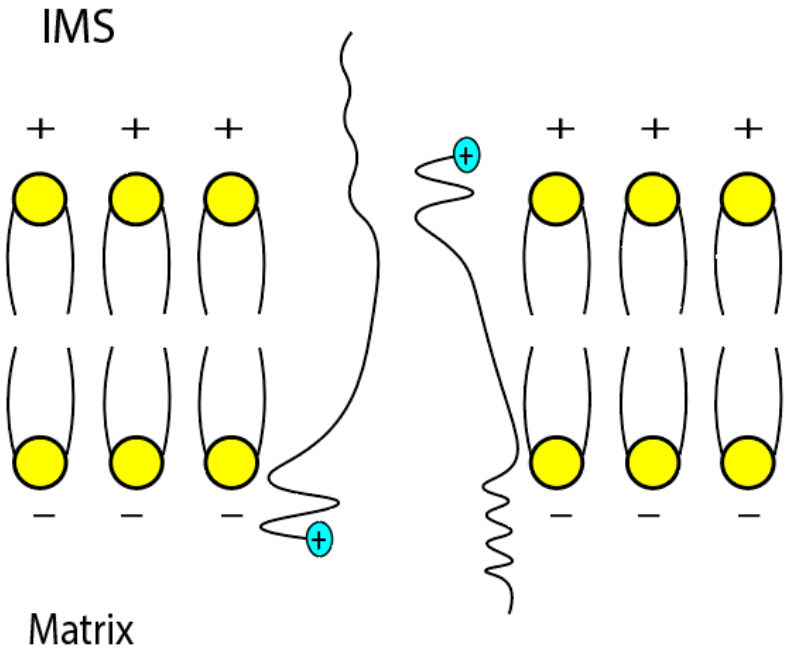

Figure 2. The figure represents the quantum tunneling of protons from the IMS and matrix sides through the inner mitochondrial membrane. The IMS protons have a higher tunneling probability illustrated by larger wave amplitude if they are compared with the waves of the matrix protons.

The quantum tunneling of protons in the IMS side through the IMM itself can be calculated by the following equation:

$$T_{IMS(IMM)} = e^{\frac{-\sqrt{8m}}{\hbar}\int_{x1}^{x2}\sqrt{(\frac{G-qV_m}{L_{IMM}})x-\frac{1}{2}K_BT}dx}, \quad (5)$$

where $x_1 = \frac{\frac{1}{2}K_BT}{G-qV_m}L_{IMM}$ at which $U(x_1) = KE = \frac{1}{2}K_BT$ and $x_2 = L_{IMM}$ which is at the end of the IMM. By solving the integral in Eq (5), it becomes:

$$T_{IMS(IMM)} = e^{\frac{-\sqrt{8m}}{\hbar}\times\frac{2L_{IMM}}{3(G-qV_m)}\sqrt{(G-qV_m-\frac{1}{2}K_BT)^3}}, \quad (6)$$

2.1.2. The quantum tunneling of protons in the matrix

The matrix protons face the potential barrier of IMM itself and its electrical potential V_m and have a kinetic energy from the thermal biological environment. Therefore, the quantum tunneling of matrix protons can be calculated by the following equation:

$$T_{Matrix(IMM)} = e^{\frac{-\sqrt{8m}}{\hbar}\int_{x1}^{x2}\sqrt{(\frac{G+qV_m}{L_{IMM}}x)-\frac{1}{2}K_BT}dx}, \quad (7)$$

where $x_1 = \frac{\frac{1}{2}K_BT}{G+qV_m}L_{IMM}$ at which $U(x_1) = KE = \frac{1}{2}K_BT$ and $x_2 = L_{IMM}$ which is at the end of inner mitochondrial membrane IMM. By solving the integral in Eq (7), it becomes:

$$T_{\text{Matrix}(IMM)} = e^{\frac{-\sqrt{8m}}{\hbar}\times\frac{2L_{IMM}}{3(G+qV_m)}\sqrt{(G+qV_m-\frac{1}{2}K_BT)^3}}, \quad (8)$$

2.2. The quantum tunneling of protons through the MCF proteins

As protons can tunnel through the IMM, they can also tunnel through the barriers of the salt-bridge networks of the MCF proteins including UCPs and ANTs. Based on the molecular structure of MCF proteins, protons may tunnel through two separate barriers, unlike the tunneling through the IMM which is assumed to be one continuous barrier. See Figure 3.

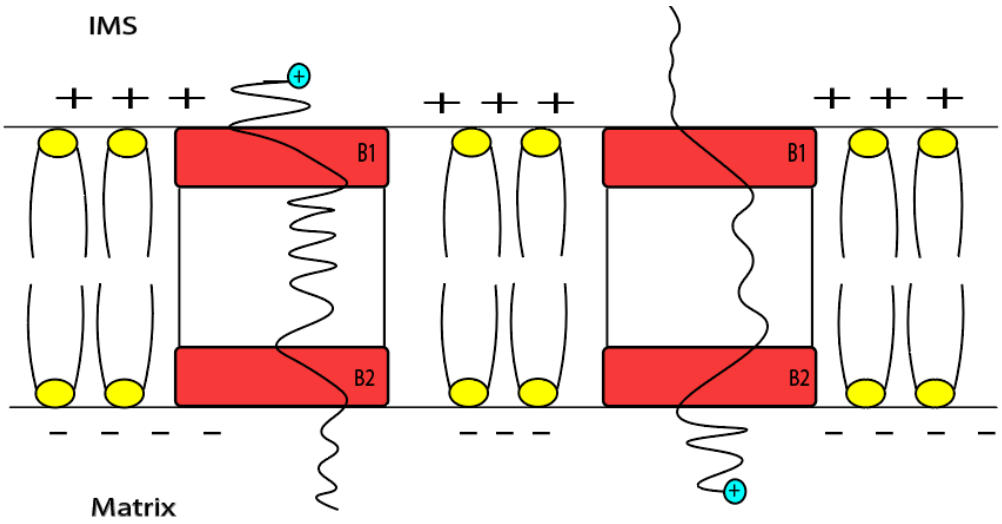

Figure 3. The figure represents the quantum tunneling of protons from the IMS and matrix sides showing their wave behavior. The quantum tunneling occurs through the two salt bridge networks at both sides that are illustrated by B1 and B2 for the IMS and matrix sides, respectively. In this model, the proton tunnels through the closed B1 and B2. The IMS protons have higher tunneling probability and higher kinetic energy illustrated by larger wave amplitude and higher wave frequency, respectively. On the other hand, the matrix protons have lower tunneling probability and lower kinetic energy illustrated by smaller wave amplitude and lower wave frequency, respectively. This will be the first model of MCF.

2.2.1. The quantum tunneling of intermembrane space IMS protons

The IMS protons encounter two potential energy barriers while tunneling through MCF proteins. The first is the salt-bridges network at the IMS side (B1) and the other is at the matrix side (B2) that are illustrated in Figure 3. The IMS protons tunnel through the potential barriers of B1 and B2, but the electrical field of IMM will decrease their barrier heights along with kinetic energy from the thermal biological environment. Accordingly, the quantum tunneling probability of IMS protons through the B1 can be calculated by the following equation:

$$T_{IMS(\mathrm{MCF-B1})} = e^{\frac{-\sqrt{8m}}{\hbar}\int_{x1}^{x2}\sqrt{(\frac{G_{B1}}{L_{B1}}-\frac{qV_m}{L_{IMM}})x-\frac{1}{2}K_BT}dx}, \quad (9)$$

where $x_1 = \dfrac{\frac{1}{2}K_BT}{(\frac{G_{B1}}{L_{B1}}-\frac{qV_m}{L_{IMM}})}$ at which $U(x_1) = KE = \frac{1}{2}K_BT$ and $x_2 = L_{B1}$ which is at the end of B1. By solving the integral in Eq (9), it becomes:

$$T_{IMS(\mathrm{MCF-B1})} = e^{\frac{-\sqrt{8m}}{\hbar}\times\frac{2}{3(\frac{G_{B1}}{L_{B1}}-\frac{qV_m}{L_{IMM}})}\sqrt{(G_{B1}-\frac{qV_mL_{B1}}{L_{IMM}}-\frac{1}{2}K_BT)^3}}, \quad (10)$$

Based on Eq (10), IMS protons tunnel through the B1 barrier with a lower barrier height compared to the original height of B1 and with kinetic energy obtained from the thermal biological environment. On the other hand, the IMS protons will tunnel through the potential barrier of B2 while getting kinetic energy from the electrical potential of IMM before reaching the B2 barrier along with the thermal kinetic energy from the surrounding environment. In addition, the electrical field across the B2 barrier will lower the barrier height of B2 for the IMS protons. Hence, the quantum tunneling probability of IMS protons through B2 can be calculated by the following equation:

$$T_{IMS(\mathrm{MCF-B2})} = e^{\frac{-\sqrt{8m}}{\hbar}\int_{x1}^{x2}\sqrt{(\frac{G_{B2}}{L_{B2}}-\frac{qV_m}{L_{IMM}})x-(\frac{qV_m(L_{IMM}-L_{B2})}{L_{IMM}}+\frac{1}{2}K_BT)}dx}, \quad (11)$$

where $x_1 = \dfrac{\frac{qV_m(L_{IMM}-L_{B2})}{L_{IMM}}+\frac{1}{2}K_BT}{(\frac{G_{B1}}{L_{B1}}-\frac{qV_m}{L_{IMM}})}$ at which $U(x_1) = KE = \frac{qV_m(L_{IMM}-L_{B2})}{L_{IMM}}+\frac{1}{2}K_BT$ and $x_2 = L_{B2}$ which is at the end of B2. By solving the integral in Eq (11), it becomes:

$$T_{IMS(\mathrm{MCF-B2})} = e^{\frac{-\sqrt{8m}}{\hbar}\times\frac{2}{3(\frac{G_{B2}}{L_{B2}}-\frac{qV_m}{L_{IMM}})}\sqrt{((G_{B2}-\frac{qV_mL_{B2}}{L_{IMM}})-\frac{qV_m(L_{IMM}-L_{B2})}{L_{IMM}}-\frac{1}{2}K_BT)^3}}, \quad (12)$$

Thus, Eq (12) becomes:

$$T_{IMS(\mathrm{MCF-B2})} = e^{\frac{-\sqrt{8m}}{\hbar}\times\frac{2}{3(\frac{G_{B2}}{L_{B2}}-\frac{qV_m}{L_{IMM}})}\sqrt{(G_{B2}-qV_m-\frac{1}{2}K_BT)^3}}, \quad (13)$$

Eventually, the quantum tunneling of IMS protons through the MCF proteins can be calculated by the following equation:

$$T_{IMS(MCF)} = T_{IMS(MCF-B1)} \times T_{IMS(MCF-B2)}, \quad (14)$$

2.2.2. The quantum tunneling of matrix protons

The matrix protons can tunnel through B1 encountering its barrier height that is increased due to the effect of the electrical field that its direction is opposite to the flow of matrix protons to the IMS side. The matrix protons attain kinetic energy from the surrounding biological environment. However, their kinetic energy will be reduced during their passage in MCF until reaching the B1 due to the influence of the opposing electrical field across the IMM. See Figure 3. Therefore, the probability of quantum tunneling through the B1 barrier can be calculated by the following equation:

$$T_{\mathrm{Matrix(MCF-B1)}} = e^{\frac{-\sqrt{8m}}{\hbar}\int_{x1}^{x2}\sqrt{(\frac{G_{B1}}{L_{B1}}+\frac{qV_m}{L_{IMM}})x-KE}dx}, \quad (15)$$

where $KE = \frac{1}{\beta}\int_{\frac{\mathrm{qV}_m(L_{IMM}-L_{B1})}{L_{IMM}}}^{\infty}(\mathrm{E}-\frac{\mathrm{qV}_m(L_{IMM}-L_{B1})}{L_{IMM}})e^{\frac{-E}{\beta}}dE$ in which E is the thermal energy, q is the charge of proton and $\beta = K_BT$; in which K_B is the Boltzmann constant and T is body temperature. By solving the integral, the kinetic energy of the matrix protons once reaching the B1 barrier can be estimated by the following equation $KE = 4.28\times10^{-21}e^{-32V_m}$ in which the prefactor 4.28×10^{-21} has the Joule (J) unit and the coefficient in the exponent (32) has the unit of V^{-1}. This equation calculates the mean thermal energy which has been lowered by the effect of the electric field of the IMM. In addition, $x_1 = \frac{KE}{(\frac{G_{B1}}{L_{B1}}+\frac{qV_m}{L_{IMM}})}$ at which $U(x_1) = KE$ and $x_2 = L_{B1}$ which is at the end of the barrier B1. By solving the integral in Eq (15), it becomes:

$$T_{\mathrm{Matrix(MCF-B1)}} = e^{\frac{-\sqrt{8m}}{\hbar}\times\frac{2}{3(\frac{G_{B1}}{L_{B1}}+\frac{qV_m}{L_{IMM}})}\sqrt{(G_{B1}+\frac{qV_mL_{B1}}{L_{IMM}}-KE)^3}}, \quad (16)$$

On the other hand, matrix protons encounter the barrier height of B2 with further increase in its height due to the electric field of IMM along with a kinetic energy attained from the thermal biological environment. Hence, the quantum tunneling of matrix protons through B2 barrier can be calculated by the following equation:

$$T_{\mathrm{Matrix(MCF-B2)}} = e^{\frac{-\sqrt{8m}}{\hbar}\int_{x1}^{x2}\sqrt{(\frac{G_{B2}}{L_{B2}}+\frac{qV_m}{L_{IMM}})x-\frac{1}{2}K_BT}dx}, \quad (17)$$

where $x_1 = \frac{\frac{1}{2}K_BT}{(\frac{G_{B2}}{L_{B2}} + \frac{qV_m}{L_{IMM}})}$ at which $U(x_1) = KE = \frac{1}{2}K_BT$ and $x_2 = L_{B2}$ which is at the end of the barrier B2. By solving the integral inEq (17), it becomes:

$$T_{\text{Matrix(MCF−B2)}} = e^{\frac{-\sqrt{8m}}{\hbar} \times \frac{2}{3(\frac{G_{B2}}{L_{B2}} + \frac{qV_m}{L_{IMM}})} \sqrt{(G_{B2} + \frac{qV_m L_{B2}}{L_{IMM}} - \frac{1}{2}K_BT)^3}}, \quad (18)$$

Eventually, the quantum tunneling of matrix protons through the MCF can be calculated by the following equation:

$$T_{Matrix(MCF)} = T_{Matrix(MCF-B1)} \times T_{Matrix(MCF-B2)}, \quad (19)$$

As a result of quantum tunneling of protons through barriers, other quantum physical quantities can be studied including the quantum unitary conductance and the quantum membrane conductance. The quantum unitary conductance is the quantum conductance due to quantum tunneling through a single barrier unit, while the quantum membrane conductance is the quantum conductance per surface area unit.

2.3. The quantum conductance of protons through the inner mitochondrial membrane IMM

The passage of IMS protons through IMM via quantum tunneling results in quantum tunneling current and quantum conductance. The quantum unitary conductance can be calculated by the following Eq [12]:

$$C_{IMS(IMM)} = \frac{q^2_{H^+}}{h} T_{IMS(IMM)}, \quad (20)$$

The quantum membrane conductance of IMM for IMS protons can be calculated by the following Eq [12]:

$$MC_{IMS(IMM)} = \frac{C_{IMS(IMM)}}{A_{(IMS)}}, \quad (21)$$

where $A_{(IMS)} = \frac{3\hbar(G - qV_m)\mathrm{L}_{IMM}}{2\sqrt{8m}\sqrt{(G - qV_m - \frac{1}{2}K_BT)^3}}$ which is the surface area unit related to tunneling barrier of IMM for IMS protons.

Similarly, the quantum unitary conductance and the quantum membrane conductance of matrix protons through the IMM can be calculated by the following equations, respectively:

$$C_{\text{Matrix}(IMM)} = \frac{q^2_{H^+}}{h} T_{\text{Matrix}(IMM)}, \quad (22)$$

$$MC_{\text{Matrix}(IMM)} = \frac{C_{\text{Matrix}(IMM)}}{A_{(\text{Matrix})}}, \tag{23}$$

where $A_{(Matrix)} = \frac{3\hbar(G+qV_m)\mathrm{L}_{IMM}}{2\sqrt{8m}\sqrt{(G+qV_m-\frac{1}{2}K_BT)^3}}$ which is the surface area unit related to tunneling barrier of IMM for matrix protons.

The surface area unit related to the tunneling barrier A can be calculated as a result of multiplying the length of the barrier L_{IMM} by the scale of length for quantum tunneling δ, hence $A = L_{IMM}\delta$ [12]. This scale of length can be deduced from equations of tunneling probability because the general equation can be represented by the following expression: $T = e^{\frac{-L}{\delta}}$ [12]. If this general equation is matched with Eqs (6) and (8), then A values for IMS and matrix protons can be determined as in Eqs (21) and (23).

2.4. The quantum conductance of protons through the MCF proteins

The quantum conductance of IMS protons through single MCF protein can be calculated by the following equation:

$$C_{IMS(MCF)} = \frac{q^2_{H^+}}{h} T_{IMS(MCF)}, \tag{24}$$

The quantum membrane conductance of IMS protons at certain density D of MCF proteins can be calculated by the following equation [31]:

$$MC_{IMS(MCF)} = C_{IMS(MCF)} \times D, \tag{25}$$

where D is the number of MCF proteins per surface area unit.

Similarly, the quantum unitary conductance and the quantum membrane conductance of matrix protons, which are mediated by MCF proteins, can be calculated by the following equations, respectively:

$$C_{\text{Matrix}(MCF)} = \frac{q^2_{H^+}}{h} T_{\text{Matrix}(MCF)}, \tag{26}$$

$$MC_{\text{Matrix}(MCF)} = C_{\text{Matrix}(MCF)} \times D, \tag{27}$$

2.5. The influence of quantum leak of protons on the electrical potential of inner mitochondrial membrane IMM

The physical origin of the electrical potential of the inner mitochondrial membrane has been explained by several approaches [32]. However, based on the electrochemical principles, two major approaches can explain the generation of the electrical potential of IMM. These two approaches are: 1) The proton flow-based approach [31] and 2) The approach of the electrostatic density of protons [32].

The proton flow-based approach states that the generation of electrical potential is generated once the balance between the chemical gradient and the gradient of electrical potential is established. This implies that the net flow of ions across the membrane is zero [31]. The proton flow-based approach is similar to the electrochemical approach that is used to calculate the membrane potential of neurons and cardiac cells using the Goldman-Hodgkin-Katz (GHK) equation [31]. On the other hand, the approach of the electrostatic density of protons states that it is the charge density of protons at both sides of the inner mitochondrial membrane that creates a voltage difference similar to the voltage difference across the capacitor [32]. Therefore, this approach does not account for the effect of proton's conductance on the membrane potential rather it accounts for the localized concentration of protons at the sides of the membrane [32]. Even though several reasons argue against the electrostatic model and assume it is inappropriate to model the bioenergetics of mitochondria [33], we use this model for comparison and to theoretically validate the critique of this model as we will explain later. In the following sections, we will investigate the influence of the quantum conductance due to proton tunneling on the electrical potential of IMM according to both approaches. There are four major pathways for proton transport across the IMM, see Figure 4. These pathways include 1) the inner mitochondrial membrane IMM itself. 2) The electron transport chain ETC protein complexes particularly complex I, complex III, and complex IV. 3) The MCF proteins including UCPs and ANTs. 4) The ATP synthase protein.

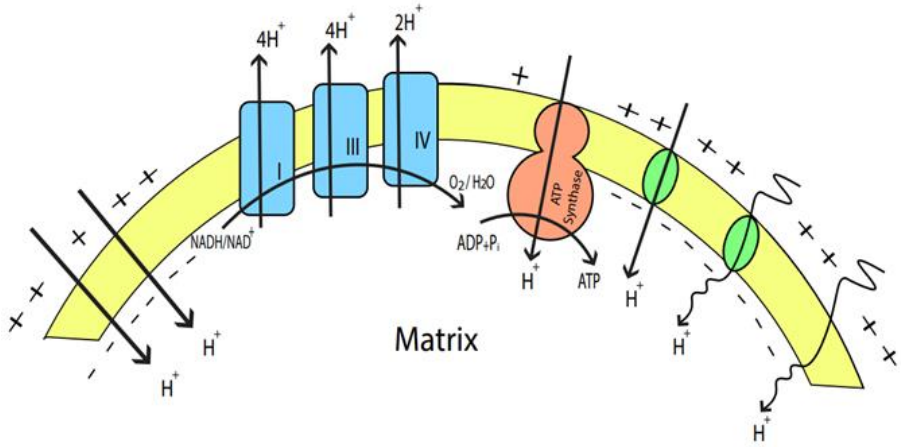

Figure 4. The figure illustrates the classical and the proposed quantum transport across the inner mitochondrial membrane IMM. The straight arrow indicates the classical transport while the wavy arrow indicates the quantum transport.

There are two possible types of transport mediated via these pathways and these include the classical transport in which the protons overcome the barrier by gaining higher energy than the barrier height. The other possible type is quantum transport which is achieved by quantum tunneling in which the protons can overcome the barrier by lower energy than the barrier height according to their quantum behavior. Accordingly, the proton transport across the leak-mediating pathways can be in the classical and quantum forms. See Figure 4. The pumping activity of ETC complexes will be assumed to be only classical transport as we focus on the quantum leak flow. In addition, the ATP synthase is mainly involved in the ADP to ATP conversion process and will not be involved in the discussion of the generation of the electrical potential of IMM.

In the first approach, the membrane potential is generated to balance the flow of protons to zero. Before involving the role of MCF proteins, two pathways contribute to the flow of protons and these are the IMM itself, and ETC protein complexes. Hence, the electrical potential of IMM is attributed to the conductance of IMM itself and the conductance of ETC proteins. The lipid bilayer membrane conductance of ions and protons is experimentally and theoretically measured by the unit of nS/cm^2 [8,26]. Assuming that the membrane conductance of the protons in the intermembrane space IMS is$1nS/cm^2 = 1\times10^{-5}$ S/m^2. The exact value of conductance is not our concern because we aim to show what the influence of quantum tunneling would be on the electrical potential using any reasonable value. Thus, the conductance of ETC proteins can be predicted using the Nernst equation:

$$\left[H^+\right]_{IMS}(MC_{IMS}) = e^{\frac{-FV_m}{RT}}\left[H^+\right]_{matrix}(MC_{matrix}), \tag{28}$$

where $\left[H^+\right]_{IMS}$ is the proton concentration in the IMS, MC_{IMS} is the classical membrane conductance of protons through the IMM, $\left[H^+\right]_{matrix}$ is the proton concentration in the matrix, MC_{matrix} is the classical membrane conductance of matrix protons due to the activity of ETC proteins, F is Faraday's constant, R is the gas constant, T is the body temperature, and V_m is the electrical potential of IMM.

By substituting the values in Table 1 in the corresponding variables in Eq (28), the conductance of the matrix protons is 5.4×10^{-2} S/m^2, which is predominantly mediated by ETC proteins. See Figure 4. The matrix protons have higher conductance than the IMS protons which is attributed to the activity of ETC proteins that favor a net proton flow to the IMS side to generate an electrical potential of 180 mV, which is positive at the IMS side relative to the matrix side. If the ETC proteins are inactivated, then the conductance of IMM will predominate and it will favor the net proton flow from the IMS side to the matrix side down the concentration gradient of protons, see Table 1. In this case, the membrane potential will be equal to the Nernst potential of protons and it will be around −50 mV, which is negative at the IMS side relative to the matrix side, which is not compatible with the bioenergetics of mitochondria. Accordingly, we will investigate the influence of the quantum tunneling transport and the classical transport on the electrical potential using the following GHK equations:

$$\left[H^+\right]_{IMS}(MC_{IMS} + MC_{Q-IMS}) = e^{\frac{-FV_m}{RT}}\left[H^+\right]_{matrix}(MC_{matrix} + MC_{Q-matrix}), \tag{29}$$

$$\left[H^+\right]_{IMS}(MC_{IMS} + MC_{C-IMS}) = e^{\frac{-FV_m}{RT}}\left[H^+\right]_{matrix}(MC_{matrix} + MC_{C-matrix}), \tag{30}$$

where MC_Q is the quantum membrane conductance mediated by IMM and/or MCF proteins and MC_C is the classical membrane conductance mediated by IMM and/or MCF proteins.

On the other hand, the second approach relies on the concentration of the localized protons not on their conductance. However, as we aim to assess the influence of the proton leak current, which is defined in terms of electrical conductance, the flow of protons will shift the electrical potential of IMM to the potential of equilibrium at which the net flow across the membrane is zero. The flow of protons will not affect the concentration of protons; hence the conductance of leak current cannot affect the membrane potential according to the electrostatic model. Therefore, the effect of conductance on membrane potential can be assessed using the GHK equation, but in this case, the conductance of ETC

proteins must be omitted because the electrostatic approach states no role for ETC conductance in the first place. In this case, if the electrostatic approach sets the membrane potential to be 180 mV and the tunneling leak current is activated, then the flow of protons can depolarize the membrane potential to the equilibrium potential determined by Nernst equation without affecting the concentration of protons according to the laws of electrochemistry. In other words, the effect of proton conductance will dominate over the effect of the electrostatic effect of protons. Accordingly, the assessment of the influence of proton leak according to the electrostatic approach will be made using the following Nernst equations:

$$\left[H^+\right]_{IMS}(MC_{Q-IMS}) = e^{\frac{-FV_m}{RT}}\left[H^+\right]_{matrix}(MC_{Q-matrix}), \tag{31}$$

$$\left[H^+\right]_{IMS}(MC_{C-IMS}) = e^{\frac{-FV_m}{RT}}\left[H^+\right]_{matrix}(MC_{C-matrix}), \tag{32}$$

3. Results

Based on the mathematical equations in the previous section, we will utilize the values of the physical parameters for mitochondria and its IMM to investigate the quantum tunneling behavior of protons, proton tunneling flow and its influence on the electrical potential of IMM (Table 1).

Table 1. The values of the physical parameters used in the study.

Parameter	Value
The thickness of IMM L_{IMM}	7×10^{-9} m
The length of the salt-bridges network $L_{B1/B2}$	1×10^{-9} m
The mass of proton	1.67×10^{-27} Kg
The protons concentration in matrix $\left[H^+\right]_{Matrix}$	1.58×10^{-5} mmol/L
The protons concentration in the IMM $\left[H^+\right]_{IMS}$	1×10^{-4} mmol/L
The electrical potential of IMM V_m	180 mV
The charge of proton q_{H^+}	1.6×10^{-19} C
The Planck constant h	6.6×10^{-34} Js
The reduced Planck constant $\hbar$	1.05×10^{-34} Js
The Boltzmann constant K_B	1.38×10^{-23} J/K
The Body temperature T	310 K
The gas constant R	8.314 J/mol.K
The Faraday's constant F	96485 C/mol

3.1. The quantum tunneling probability of protons

3.1.1. The quantum tunneling through the inner mitochondrial membrane IMM

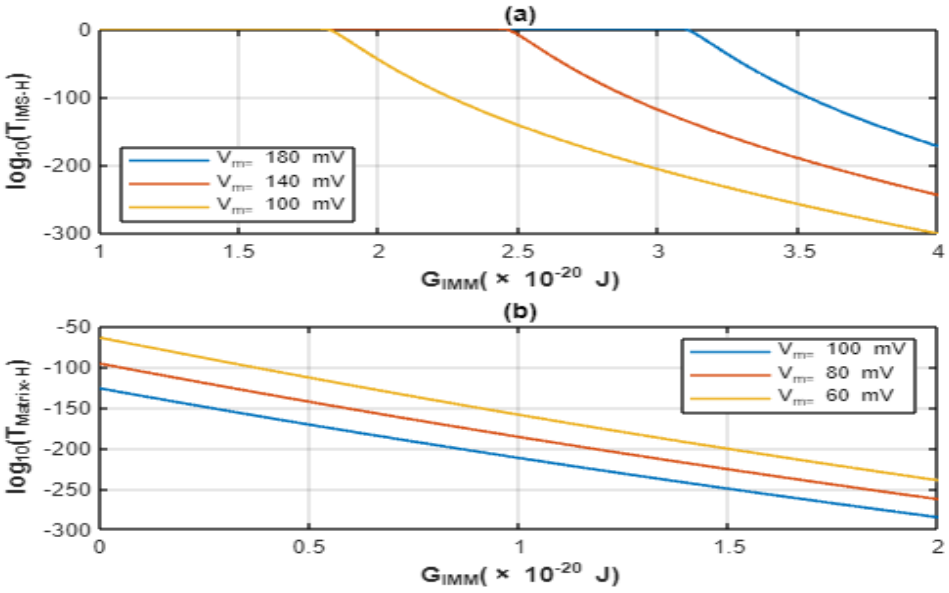

Figure 5. (a): The relationship between the barrier height of inner mitochondrial membrane IMM and the logarithm of the tunneling probability for the IMS protons. **(b):** The relationship between the barrier height of the inner mitochondrial membrane IMM and the logarithm of the tunneling probability for the matrix protons. The investigation is made at different values for the electrical potential of IMM.

Based on Eqs (6) and (8), the relationship between the barrier height of IMM and the quantum tunneling probability of protons at different values of the electrical potential of IMM can be investigated (Figure 5).

3.1.2. The quantum tunneling through the mitochondrial carrier superfamily MCF

Based on Eqs (10) and (16), the relationship between the barrier height of B1 and the quantum tunneling probability of protons at different values of the electrical potential of IMM can be investigated. See Figure 6.

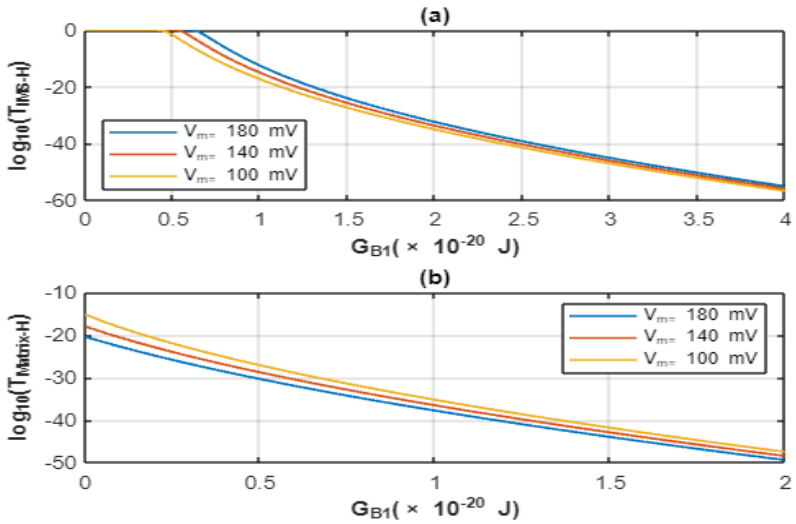

Figure 6. (a): The relationship between the barrier height of B1 and the logarithm of the tunneling probability of IMS protons through B1 barrier. **(b):** The relationship between the barrier height of B1 and the logarithm of the tunneling probability of matrix protons through B1 barrier. The investigation is made at different values for the electrical potential of IMM and assuming that B1 barrier is closed and the B2 barrier is open.

Based on Eqs (13) and (18), the relationship between the barrier height of B2 and the quantum tunneling probability of protons at different values of the electrical potential of IMM can be investigated (Figure 7).

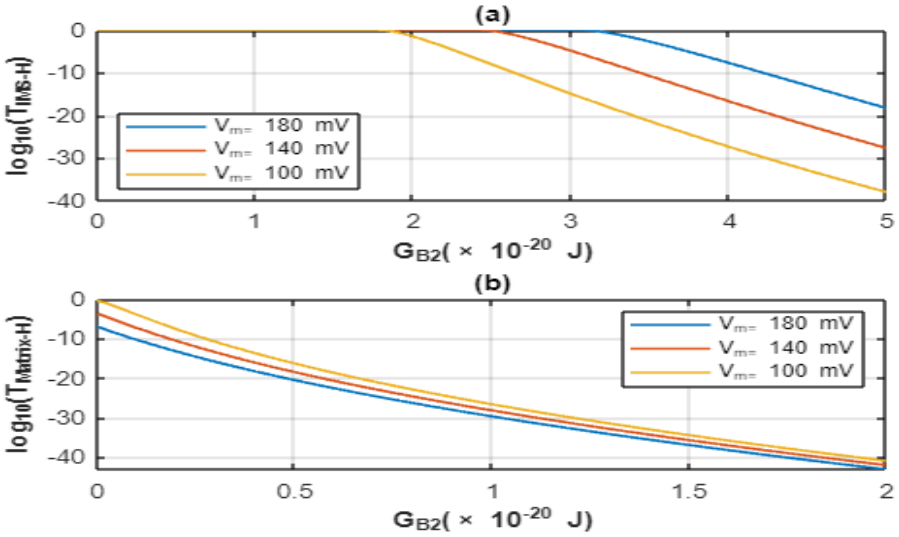

Figure 7. (a): The relationship between the barrier height of B2 and the logarithm of the tunneling probability of IMS protons through B2 barrier. **(b):** The relationship between the barrier height of B2 and the logarithm of the tunneling probability through B2 barrier. The investigation is made at different values for the electrical potential of IMM and assuming that B1 barrier is open and the B2 barrier is closed.

Based on Eqs (14) and (19), the relationship between the barrier height of B1 and B2 and the tunneling probability of protons at different values of the electrical potential of IMM can be investigated (Figure 8).

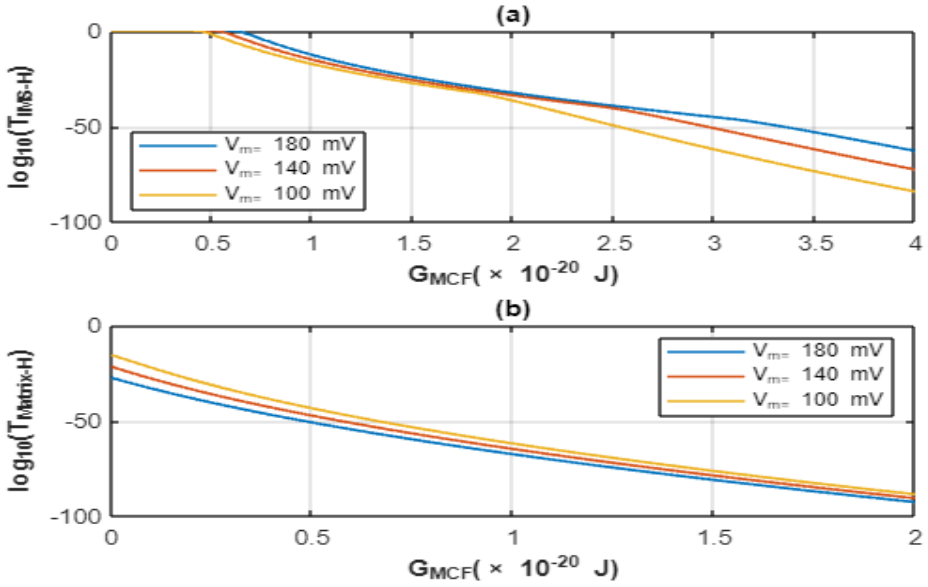

Figure 8. (a): The relationship between the barrier height of MCF (both B1 and B2 are closed) and the logarithm of tunneling probability of IMS protons through B1 and B2 barriers. **(b):** The relationship between the barrier height of MCF and the logarithm of tunneling probability of matrix protons through B1 and B2 barriers.

3.2. The quantum unitary conductance of protons

3.2.1. The quantum unitary conductance of the inner mitochondrial membrane IMM

Based on Eqs (20) and (22), the relationship between the barrier height of IMM and its quantum unitary conductance at different values of its electrical potential can be investigated (Figure 9).

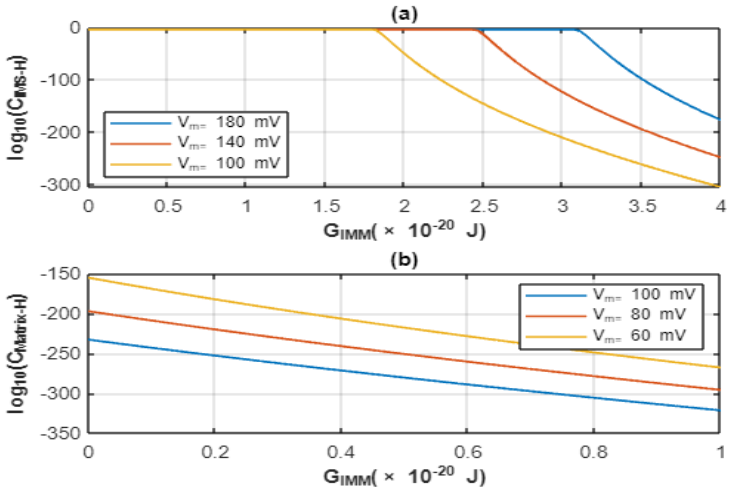

Figure 9. (a): The relationship between the barrier height of the inner mitochondrial membrane IMM and the logarithm of the unitary conductance of IMS protons. **(b):** The relationship between the barrier height of the inner mitochondrial membrane IMM and the logarithm of the unitary conductance of matrix protons. The investigation is made at different values for the electrical potential of the IMM.

3.2.2. The quantum unitary conductance of the mitochondrial carrier superfamily MCF

Based on Eqs (24) and (26), the relationship between the barrier height of B1 and the quantum unitary conductance of MCF at different values of the electrical potential of IMM can be investigated (Figure 10).

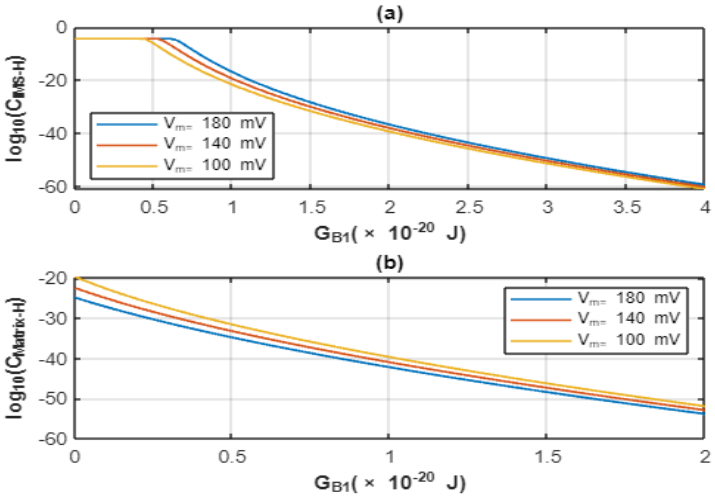

Figure 10. (a): The relationship between the barrier height of B1 barrier and the logarithm of the unitary quantum conductance of IMS protons. **(b):** The relationship between the barrier height of B1 barrier and the logarithm of the unitary quantum conductance of matrix protons. The investigation is made at different values for the electrical potential of IMM.

Based on Eqs (24) and (26), the relationship between the barrier height of B2 and the quantum unitary conductance of protons at different values of the electrical potential of IMM can be investigated (Figure 11).

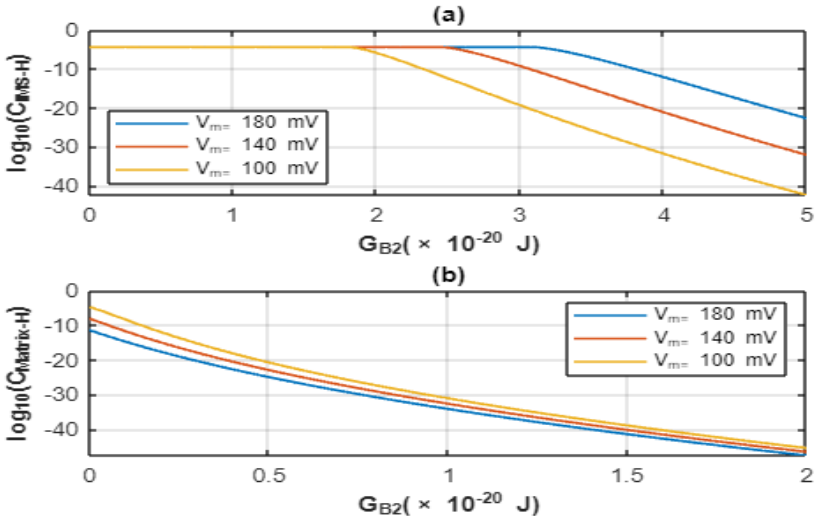

Figure 11. (a): The relationship between the barrier height of the B2 barrier and the logarithm of the unitary quantum conductance of IMS protons. **(b):** The relationship between the barrier height of the B2 barrier and the logarithm of the unitary quantum conductance of matrix protons. The investigation is made at different values of electrical potential of the IMM.

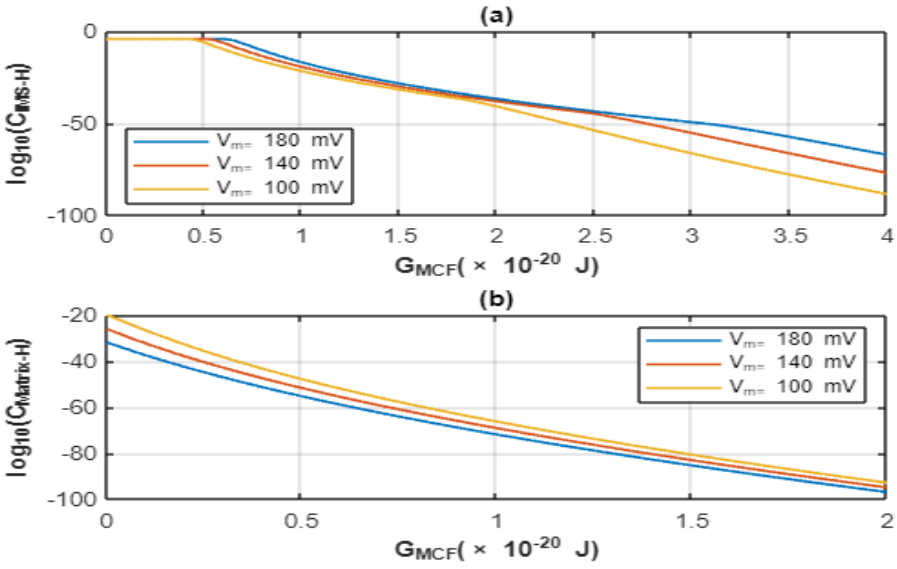

Figure 12. (a): The relationship between the barrier height of MCF (both B1 and B2 are closed) and the logarithm of the unitary quantum conductance of IMS protons. **(b):** The relationship between the barrier height of MCF and the logarithm of the unitary quantum conductance of matrix protons. The investigation is made at different values for the electrical potential of IMM.

Based on Eqs (24) and (26), the relationship between the barrier height of B1 and B2 or so called the barrier height of MCF and its quantum unitary conductance at different values of the electrical potential of IMM can be investigated (Figure 12).

3.3. The quantum membrane conductance of protons

3.3.1. The quantum membrane conductance of the inner mitochondrial membrane IMM

Based on Eqs (21) and (23), the relationship between the barrier height of the IMM and the quantum membrane conductance of protons at different values of the electrical potential of IMM can be investigated (Figure 13).

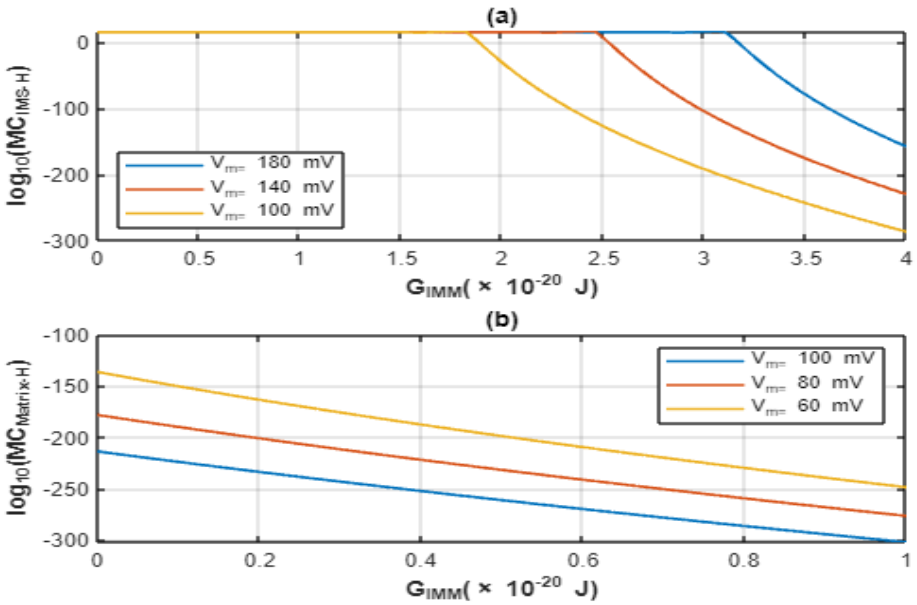

Figure 13. (a): The relationship between the barrier height of the inner mitochondrial membrane IMM and the logarithm of the quantum membrane conductance of IMS protons. **(b):** The relationship between the barrier height of the inner mitochondrial membrane IMM and the logarithm of the membrane quantum conductance of matrix protons. The investigation is made at different values for the electrical potential of IMM.

3.3.2. The quantum membrane conductance via quantum tunneling through the mitochondrial carrier superfamily MCF

Based on Eqs (25) and (27), the relationship between the barrier height of B1 and the quantum membrane conductance can be investigated at MCF protein density of 10^{14} m^{-2} and at different values of the electrical potential of IMM (Figure 14).

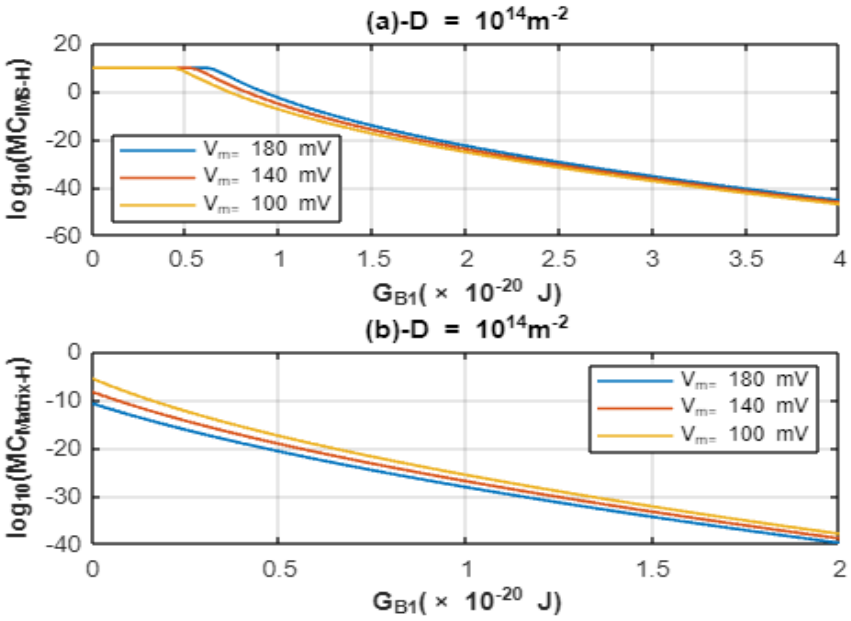

Figure 14. (a): The relationship between the barrier height of B1 barrier and the logarithm of the quantum membrane conductance of IMS protons. **(b):** The relationship between the barrier height of B1 and the logarithm of the quantum membrane conductance of matrix protons. The investigation is made at different values for the electrical potential of the IMM and protein density $D = 10^{14}\,\mathrm{m}^{-2}$.

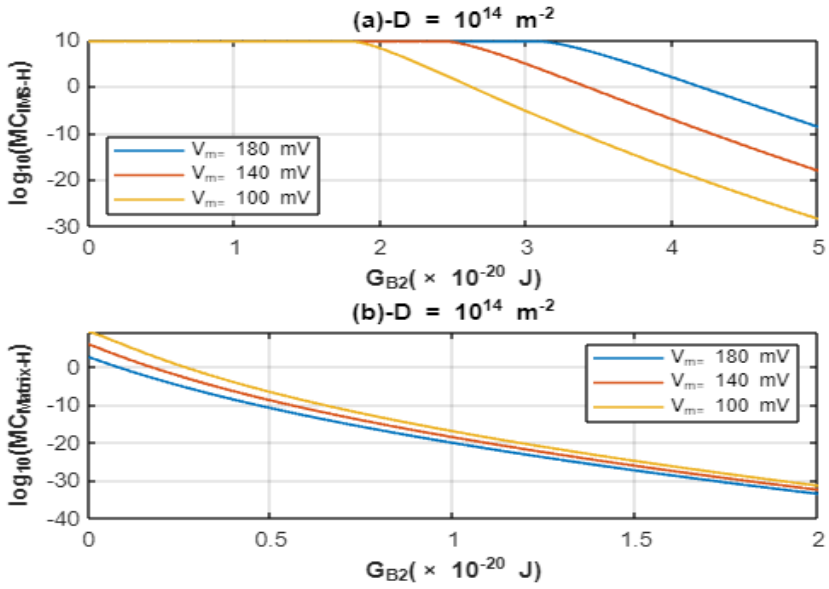

Figure 15. (a): The relationship between the barrier height of B2 barrier and the logarithm of the quantum membrane conductance of IMS protons. **(b):** The relationship between the barrier height of B2 and the logarithm of the quantum membrane conductance of matrix protons. The investigation is made at different values for the electrical potential of the IMM and protein density $D = 10^{14}\,\mathrm{m}^{-2}$.

Based on Eqs (25) and (27), the relationship between the barrier height of B2 and the quantum membrane conductance can be investigated at MCF protein density of 10^{14} m^{-2} and at different values of the electrical potential of IMM (Figure 15).

Based on Eqs (25) and (27), the relationship between the barrier height of B1 and B2 and the quantum membrane conductance can be investigated at MCF protein density of 10^{14} m^{-2} and at different values of the electrical potential of the IMM (Figure 16).

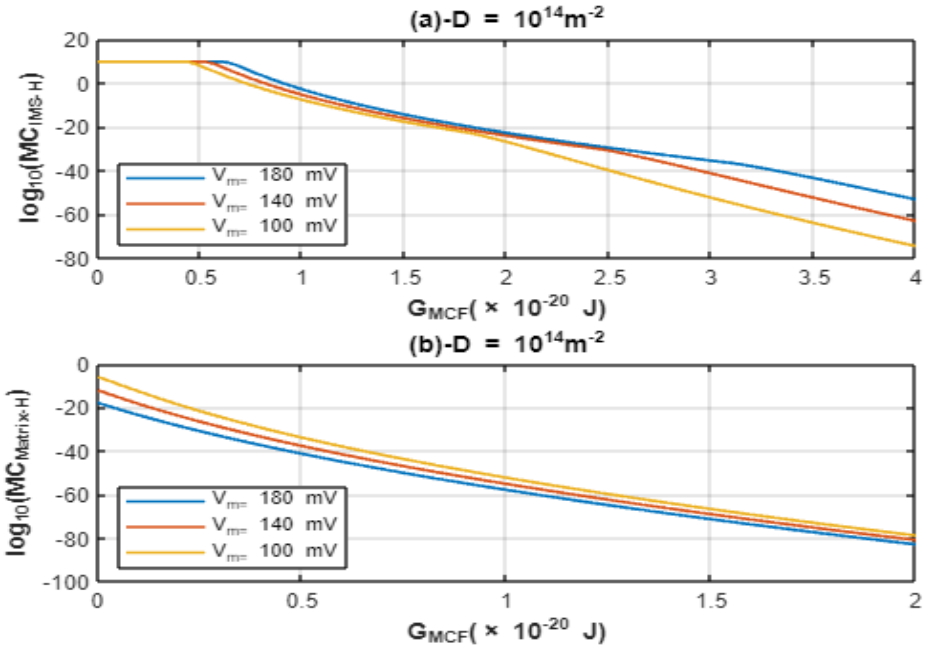

Figure 16. (a): The relationship between the barrier height of MCF (both B1 and B2 barriers are closed) and the logarithm of the quantum membrane conductance of IMS protons. **(b):** The relationship between the barrier height of MCF and the logarithm of the quantum membrane conductance of matrix protons. The investigation is made at different values of electrical potential and at protein density value $D = 10^{14}\,m^{-2}$.

3.4. The influence of the proton quantum tunneling on the electrical potential of IMM

The quantum tunneling of protons generates a proton flow and a quantum conductance. Therefore, the proton tunneling can affect the electrical potential of IMM and as a result, it can affect the ATP and ROS production. Since the MCF proteins alternate between the two states of the salt-bridge network (IMS state and matrix state) during proton flow and the regulators such as fatty acids can act on one state rather than the two states [3−5], several models can be proposed to investigate the quantum tunneling of protons through the MCF proteins (Figures 3 and 17).

There are five models of proton quantum tunneling: 1) both barriers B1 and B2 are closed and protons tunnel through them, see Figure 3. 2) B1 barrier is closed for protons at both sides of IMM, hence proton tunneling occurs through the B1 barrier, and there will be a classical transport through the B2 barrier, see Figure 17a. 3) B2 is closed for protons at both sides of IMM, hence proton tunneling occurs through the B2 barrier and there will be a classical transport through the B1 barrier, see Figure

17b. 4) B1 is closed for IMS protons while B2 is closed for matrix protons, hence IMS protons tunnel through the B1 barrier and are classically transported through the B2 barrier and matrix protons tunnel through the B2 barrier and are classically transported through the B1 barrier, see Figure 17c. 5) B2 is closed for IMS protons while B1 is closed for matrix protons, hence IMS protons tunnel through the B2 barrier and are classically transported through the B1 barrier and matrix protons tunnel through the B1 barrier and are classically transported through the B2 barrier (Figure 17d).

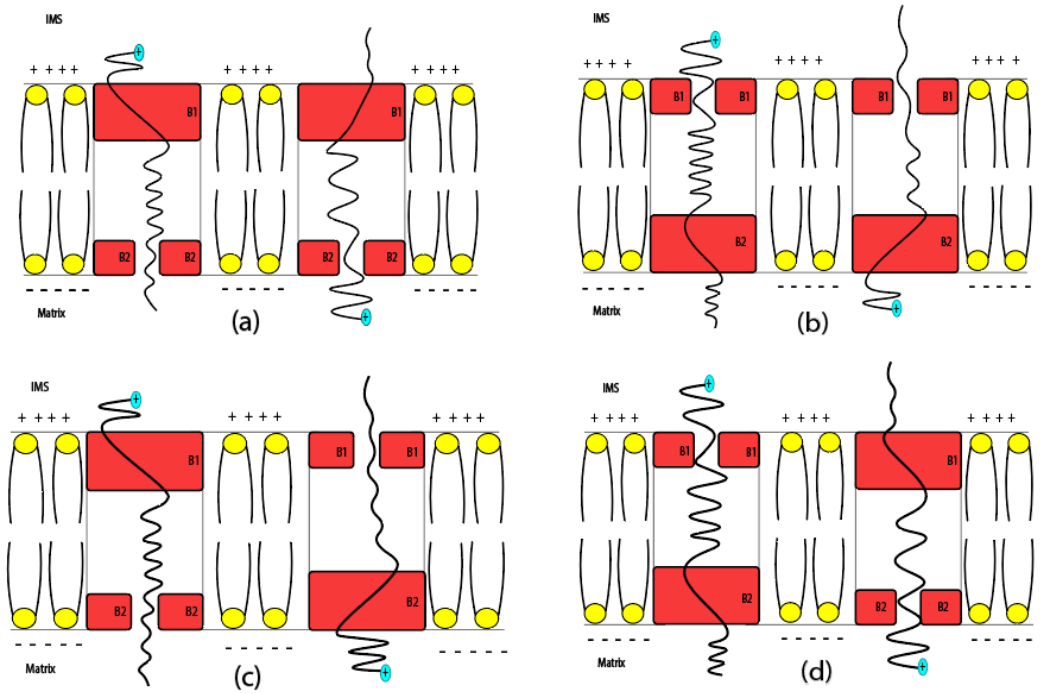

Figure 17. The figure represents four possible models for the states of B1 and B2 barriers and the corresponding quantum tunneling process showing their wave behavior. **(a):** The second model of MCF. **(b):** The third model of MCF. **(c):** The fourth model of MCF. **(d):** The fifth model of MCF.

As we explained before, there are two approaches to investigating the influence of proton tunneling on the electrical potential of IMM: 1) The proton flow–based approach in which the membrane potential is generated due to the electrical conductance of IMM for protons similar to the potential generation in neurons and cardiac cells. 2) The approach of electrostatic density of protons in which the electrostatic accumulation of protons at the IMS side generates the difference in the voltage across the membrane similar to the capacitor. Therefore, the electrostatic approach does not depend on the conductance of protons. In the present study, we aim to show how proton tunneling may affect the electrical potential according to the two approaches and what the differences between them are.

To assess the influence of quantum tunneling of protons through the IMM on its electrical potential according the proton flow-based approach, the quantum version of Goldman-Hodgkin-Katz equation is used [34]:

$$\left[H^{+}\right]_{IMS}\left(MC_{IMS}+MC_{Q-IMS(IMM)}\right)=e^{\frac{-FV_m}{RT}}\left[H^{+}\right]_{matrix}\left(MC_{matrix}+MC_{Q-matrix(IMM)}\right) \quad (33)$$

The relationship between the energy barrier height of the IMM and its membrane potential can be investigated based on Eq (33) (Figure 18).

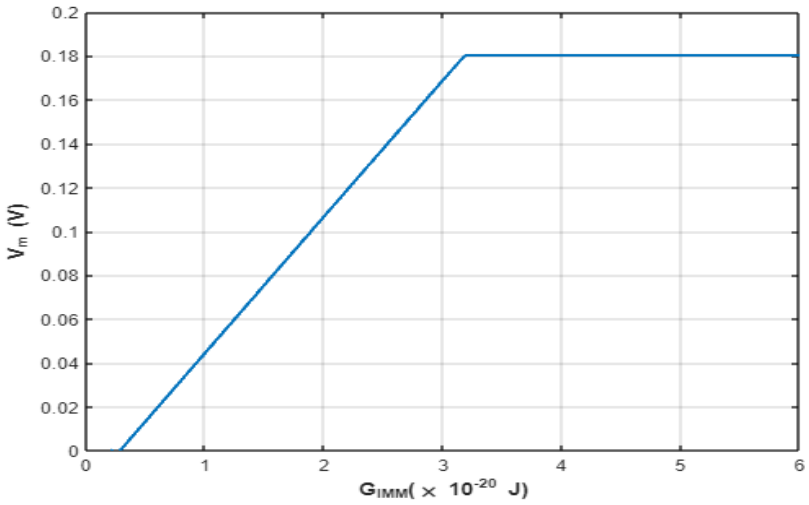

Figure 18. The figure represents the relationship between the barrier height of the inner mitochondrial membrane IMM and the electrical potential of IMM. This relationship is made according to the proton flow-based approach.

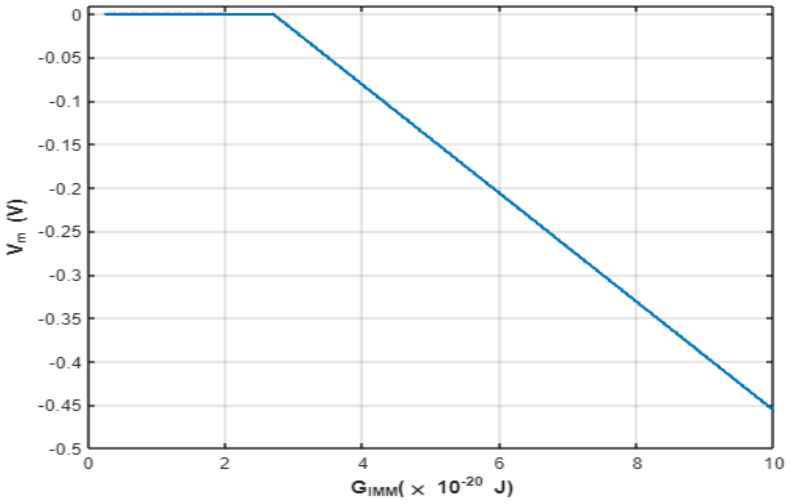

Figure 19. The figure represents the relationship between the barrier height of the inner mitochondrial membrane IMM and the electrical potential of the IMM. The investigation is made according to the electrostatic approach.

To assess the influence of the proton quantum tunneling through the IMM on its electrical potential according to the approach of electrostatic density, the Nernst equation can be used involving the quantum conductance of protons:

$$\left[H^+\right]_{IMS}(MC_{Q-IMS(IMM)}) = e^{\frac{-FV_m}{RT}}\left[H^+\right]_{matrix}(MC_{Q-matrix(IMM)}), \quad (34)$$

According to Eq (34), the quantum tunneling flow across the IMM will be balanced at the equilibrium point of Nernst potential at which the net flow across the IMM is zero. The relationship between the barrier height of IMM and its electrical potential can be investigated based on Eq (34) (Figure 19).

3.5. The influence of quantum leak current of protons through the MCF proteins on the membrane potential of IMM

The influence of the protons quantum tunneling through both barriers B1 and B2 of MCF proteins on the electrical potential of IMM according to the proton flow-based approach can be investigated using the following GHK equation:

$$\left[H^+\right]_{IMS}\left(MC_{IMS}+MC_{Q-IMS(\mathrm{MCF-B1B2})}\right)=e^{\frac{-FV_m}{RT}}\left[H^+\right]_{matrix}\left(MC_{matrix}+MC_{Q-matrix(\mathrm{MCF-B1B2})}\right) \quad (35)$$

The relationship between the barrier height of both barriers B1 and B2 or so called the barrier height of MCF and the electrical potential of IMM can be investigated based on Eq (35) (Figure 20).

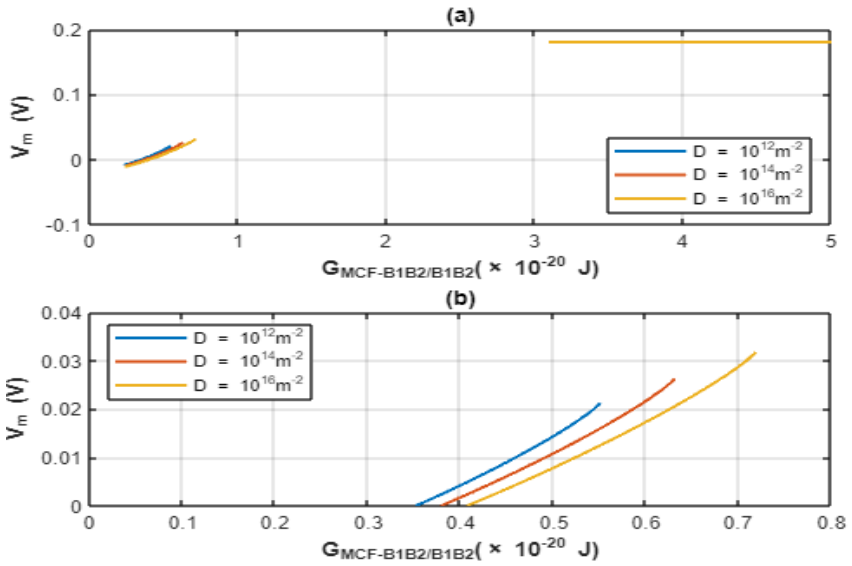

Figure 20. The figure represents the relationship between the barrier height of the MCF and the electrical potential of the inner mitochondrial membrane potential IMM. **(a):** the figure shows that there is no real solution when the both barriers B1 and B2 are closed within the range values of barrier height between around 1 and 3. **(b):** the relationship is investigated with a range of barrier height less than 1 in which real solution for the membrane potential can be found. This relationship is made according to the proton flow-based approach.

On the other hand, the influence of the protons quantum tunneling through both barriers, as in the first model, on the electrical potential of IMM according to the approach of electrostatic density of protons can be investigated using the Nernst equation:

$$\left[H^{+}\right]_{IMS}(MC_{Q-IMS(\mathrm{MCF-B1B2})}) = e^{\frac{-FV_m}{RT}}\left[H^{+}\right]_{matrix}(MC_{Q-matrix(\mathrm{MCF-B1B2})}) \tag{36}$$

The relationship between the barrier height of MCF and the electrical potential of IMM can be investigated based on Eq (36) (Figure 21).

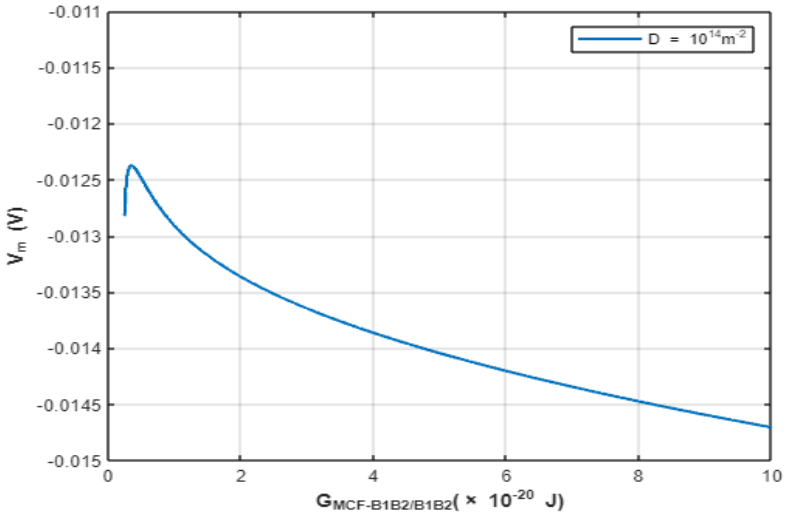

Figure 21. The figure represents the relationship between the barrier height of the MCF and the electrical potential of IMM. The investigation is made according to the electrostatic approach. One value of MCF density is chosen because the graph will not change by changing D values.

Figure 20 and Figure 21 investigated the influence of protons quantum tunneling through MCF proteins according to the first model of MCF that is illustrated in Figure 3.

In the second model of MCF, its influence on the electrical potential of IMM according to the proton flow-based approach and the approach of electrostatic density can be investigated by the following equations, respectively:

$$\left[H^{+}\right]_{IMS}(MC_{IMS} + MC_{Q-IMS(\mathrm{MCF-B1})}) = e^{\frac{-FV_m}{RT}}\left[H^{+}\right]_{matrix}(MC_{matrix} + MC_{Q-matrix(\mathrm{MCF-B1})}), \tag{37}$$

$$\left[H^{+}\right]_{IMS}(MC_{Q-IMS(\mathrm{MCF-B1})}) = e^{\frac{-FV_m}{RT}}\left[H^{+}\right]_{matrix}(MC_{Q-matrix(\mathrm{MCF-B1})}), \tag{38}$$

Based on Eqs (37) and (38), the relationship between the barrier height of B1 barrier and the electrical potential of IMM can be investigated (Figure 22).

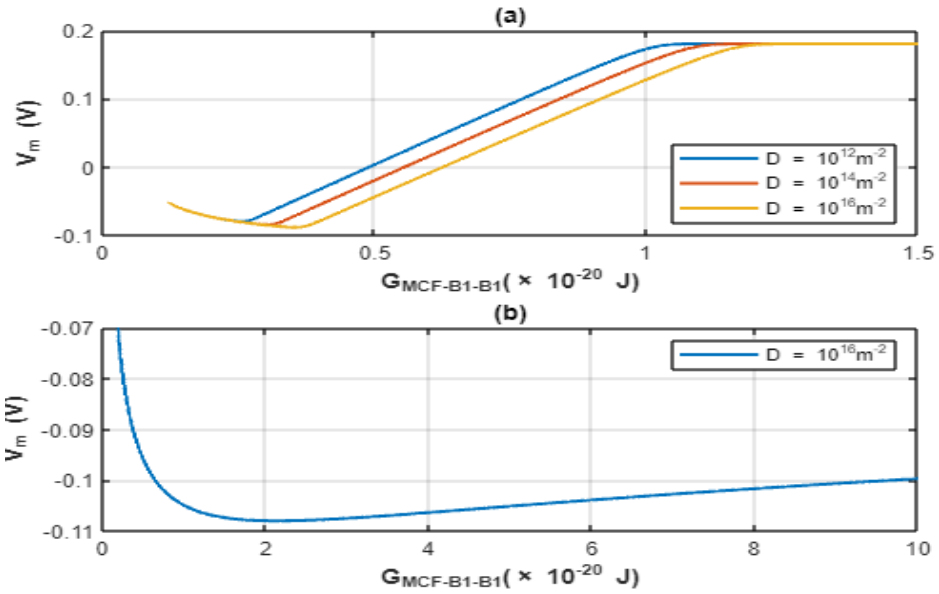

Figure 22. (a): the figure represents the relationship between the barrier height of B1 for protons at both sides and the electrical potential of the inner mitochondrial membrane IMM. The relationship is made according to the proton flow-based approach and at different values of protein density**. (b):** the figure represents the relationship between the barrier height of B1 for protons at both sides and the electrical potential of the inner mitochondrial membrane IMM. The relationship is made according to the electrostatic approach and at different values of protein density. One value of MCF density is chosen because the graph will not change by changing *D* values.

In the third model of MCF, its influence on the electrical potential of IMM according to the proton flow-based approach and the approach of electrostatic density can be investigated by the following equations, respectively:

$$\left[H^+\right]_{IMS}\left(MC_{IMS}+MC_{Q-IMS(\mathrm{MCF-B2})}\right)=e^{\frac{-FV_m}{RT}}\left[H^+\right]_{matrix}\left(MC_{matrix}+MC_{Q-matrix(\mathrm{MCF-B2})}\right), \quad (39)$$

$$\left[H^+\right]_{IMS}\left(MC_{Q-IMS(\mathrm{MCF-B2})}\right)=e^{\frac{-FV_m}{RT}}\left[H^+\right]_{matrix}\left(MC_{Q-matrix(\mathrm{MCF-B2})}\right) \quad (40)$$

Based on Eqs (39) and (40), the relationship between the barrier height of B2 barrier and the electrical potential of IMM can be investigated (Figure 23).

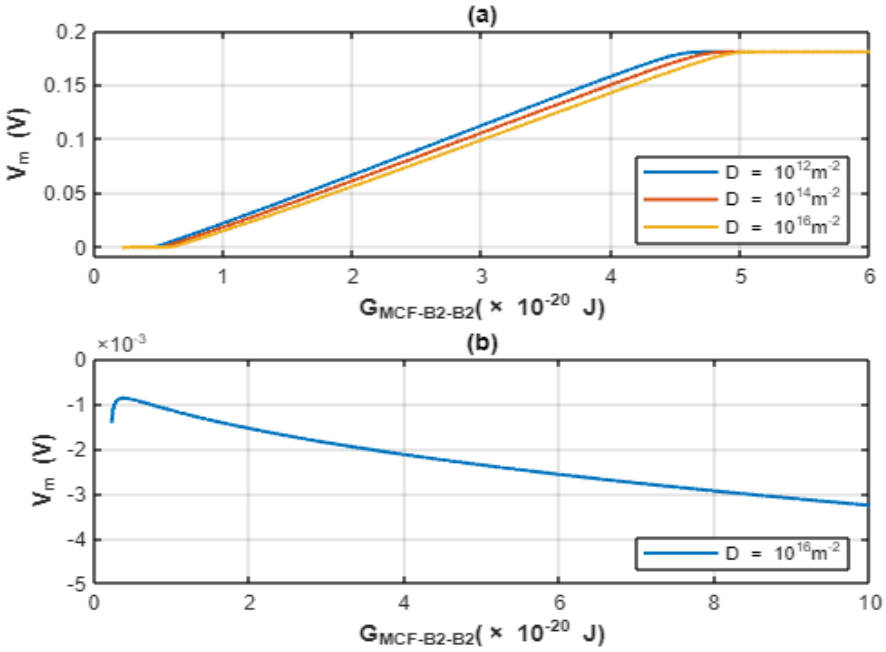

Figure 23. The figure represents the relationship between the barrier height of B2 for protons at both sides and the electrical potential of the inner mitochondrial membrane IMM. **(a):** The relationship is made according to the proton flow-based approach and at different values of protein density. **(b):** The relationship is made according to the electrostatic approach. One value of MCF density is chosen because the graph will not change by changing *D* values.

In the fourth model of MCF, its influence on the electrical potential of IMM according to the proton flow-based approach and the approach of electrostatic density can be investigated by the following equations, respectively:

$$\left[H^+\right]_{IMS}(MC_{IMS}+MC_{Q-IMS(\mathrm{MCF-B1})})=e^{\frac{-FV_m}{RT}}\left[H^+\right]_{matrix}(MC_{matrix}+MC_{Q-matrix(\mathrm{MCF-B2})}), \quad (41)$$

$$\left[H^+\right]_{IMS}(MC_{Q-IMS(\mathrm{MCF-B1})})=e^{\frac{-FV_m}{RT}}\left[H^+\right]_{matrix}(MC_{Q-matrix(\mathrm{MCF-B2})}) \quad (42)$$

Based on Eqs (41) and (42), the relationship between the barrier height of B1 or B2 barrier and the electrical potential of IMM can be investigated (Figure 24).

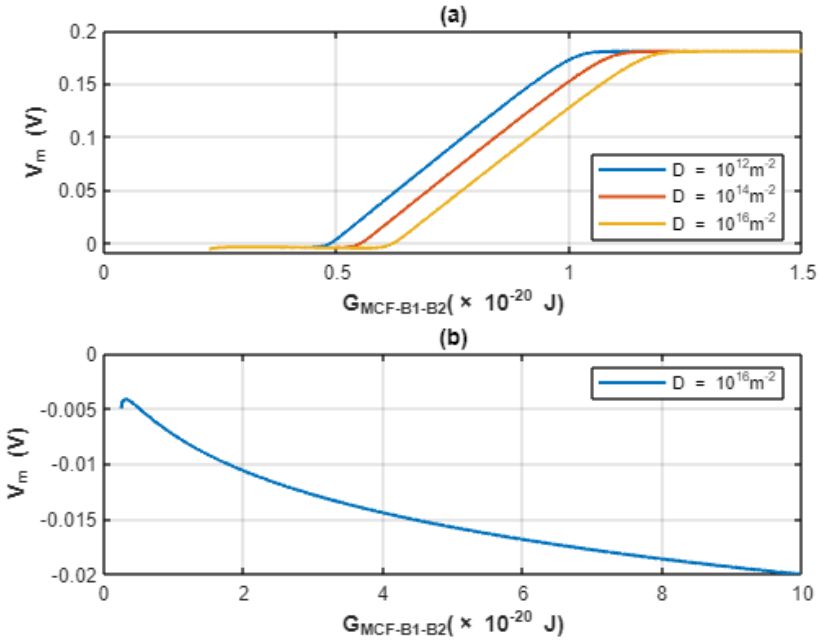

Figure 24. The figure represents the relationship between the barrier height of B1 for IMS protons and B2 for matrix protons and the electrical potential of the inner mitochondrial membrane IMM. **(a):** The relationship is made according to the proton flow-based approach and at different values of protein density. **(b):** the relationship is made according to the electrostatic approach. One value of MCF density is chosen because the graph will not change by changing *D* values.

In the fifth model of MCF, its influence on the electrical potential of IMM according to the proton flow-based approach and the approach of electrostatic density can be investigated by the following equations, respectively:

$$\left[H^+\right]_{IMS}(MC_{IMS}+MC_{Q-IMS(\mathrm{MCF-B2})})=e^{\frac{-FV_m}{RT}}\left[H^+\right]_{matrix}(MC_{matrix}+MC_{Q-matrix(\mathrm{MCF-B1})}), \tag{43}$$

$$\left[H^+\right]_{IMS}(MC_{Q-IMS(\mathrm{MCF-B2})})=e^{\frac{-FV_m}{RT}}\left[H^+\right]_{matrix}(MC_{Q-matrix(\mathrm{MCF-B1})}), \tag{44}$$

Based on Eqs (43) and (44), the relationship between the barrier height of B1 or B2 barrier and the electrical potential of IMM can be investigated (Figure 25).

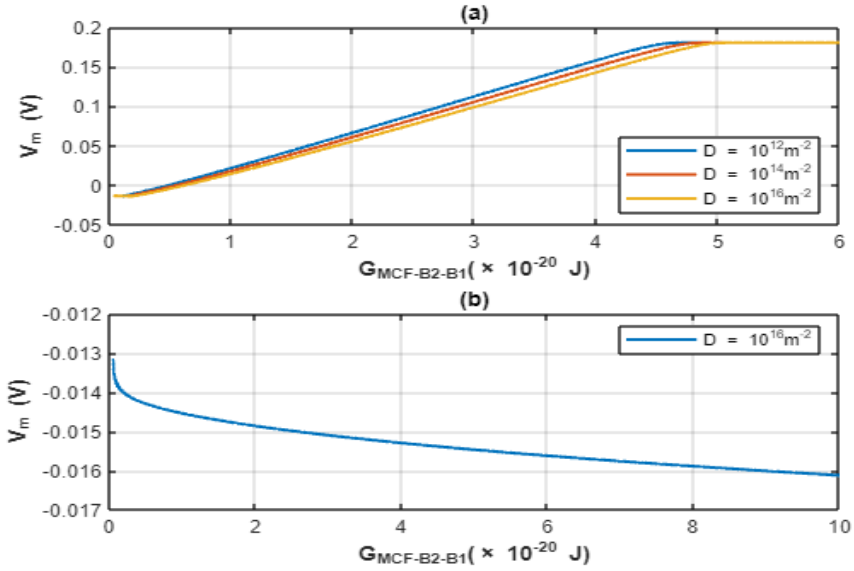

Figure 25. The figure represents the relationship between the barrier height of B2 for IMS protons and B1 for matrix protons. **(a):** The relationship is made according to the proton flow-based approach and at different values of protein density**. (b):** The relationship is made according to the electrostatic approach. One value of MCF density is chosen because the graph will not change by changing *D* values.

3.6. The influence of the classical flow of protons on the electrical potential of the IMM

The previous investigations focused on the influence of the tunneling leak flow of protons on the electrical potential of IMM. However, it is important to assess the effect of the classical leak of protons. The statistical Boltzmann distribution can be used to study the influence of the classical transport of protons via MCF proteins. The effect of the classical transport of protons through open MCF proteins on the electrical potential of IMM can be investigated using the statistical Boltzmann distribution according to the proton flow-based approach and the approach of electrostatic density using the following equations, respectively:

$$\left[H^+\right]_{IMS}\left(MC_{IMS}+\frac{DC_{C-MCF}}{1+e^{\frac{2G_{B1/B2}}{K_BT}}}\right)=e^{\frac{-FV_m}{RT}}\left[H^+\right]_{matrix}\left(MC_{matrix}+\frac{DC_{C-MCF}}{1+e^{\frac{2G_{B1/B2}}{K_BT}}}\right), \tag{45}$$

$$\left[H^+\right]_{IMS}\left(\frac{DC_{C-MCF}}{1+e^{\frac{2G_{B1/B2}}{K_BT}}}\right)=e^{\frac{-FV_m}{RT}}\left[H^+\right]_{matrix}\left(\frac{DC_{C-MCF}}{1+e^{\frac{2G_{B1/B2}}{K_BT}}}\right), \tag{46}$$

where C_{MCF} is the classical unitary conductance of MCF protein when proton flows through an open state of B1 and B2 barriers. The barrier height of either B1 or B2 is multiplied by 2 is to indicate that at least two times the barrier height of B1 or B2 are required to achieve a full classical transport through MCF protein assuming the barrier height of B1 and B2 are the same for the sake of the mathematical simplicity. Up to authors' knowledge, the range values of C_{C-MCF} has not been determined yet, but we can assume a value of 10^{-17} S to fit the membrane conductance of protons with a unit of nS/cm^2 along with *D* values in the range of $10^{12}-10^{16}$ m^{-2}, which correspond to $1-10^4$

protein/ μm^2 .

Based on Eqs (45) and (46), the relationship between the barrier height of B1/B2 and the electrical potential can be investigated (Figure 26).

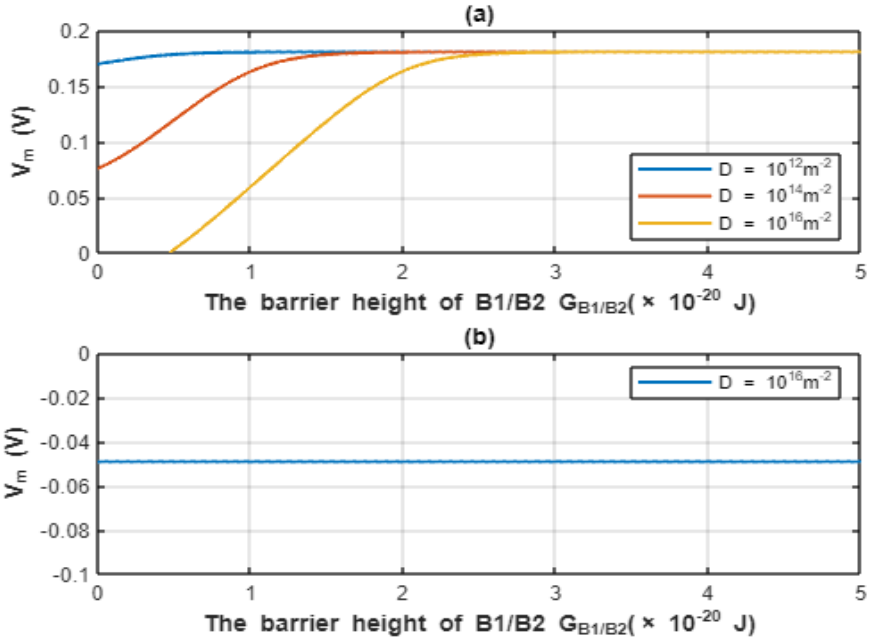

Figure 26. The figure investigates the influence of the classical flow of protons on the electrical potential of inner mitochondrial membrane IMM. **(a):** The relationship between the barrier height of B1 or B2 barrier and the electrical potential of the inner mitochondrial membrane IMM based on the proton flow-based approach. **(b):** The relationship between the barrier height of B1 or B2 barrier and the electrical potential of the inner mitochondrial membrane IMM based on the approach of electrostatic density of protons. One value of MCF density is chosen because the graph will not change by changing *D* values.

Furthermore, we can investigate the effect of the classical transport of protons on the electrical potential of IMM in terms of the classical conductance values of protons. These conductance values are either for the IMM itself or the MCF proteins using the following equations for the proton flow-based approach and the approach of electrostatic density, respectively:

$$\left[H^+\right]_{IMS}(MC_{IMS}+MC_{C-IMM/MCF}) = e^{\frac{-FV_m}{RT}}\left[H^+\right]_{matrix}(MC_{matrix}+MC_{C-IMM/MCF}), \tag{47}$$

$$\left[H^+\right]_{IMS}(MC_{C-IMM/MCF}) = e^{\frac{-FV_m}{RT}}\left[H^+\right]_{matrix}(MC_{C-IMM/MCF}), \tag{48}$$

Based on Eqs (47) and (48), the relationship between the classical conductance of protons and the electrical potential of IMM can be investigated (Figure 27).

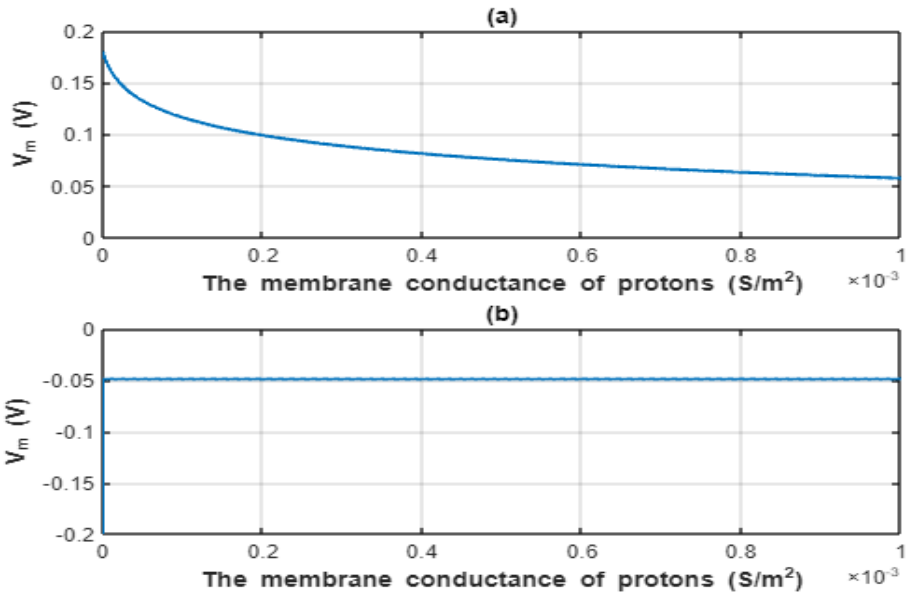

Figure 27. The figure represents the relationship between the membrane conductance of protons and the electrical potential of IMM according to the classical transport of protons. **(a):** The relationship is made according to the proton flow-based approach. **(b):** the relationship is made according to the electrostatic approach.

3.7. The tunneling leaky current of protons

In the context of our present study, it is crucial to quantify the proton leak current mediated by quantum tunneling. The tunneling leak current can be calculated based on the conductance values using the following equation:

$$I_Q = C_Q V_m, \tag{49}$$

where I_Q is tunneling leak current, C_Q is the unitary quantum conductance discussed earlier and V_m is the electrical potential of IMM. The unit of current that will be used is Ampere (A).

Based on Eq (49), the relationship between the electrical potential of IMM and the tunneling leak current can be studied for the proposed barriers (Figures 28−31).

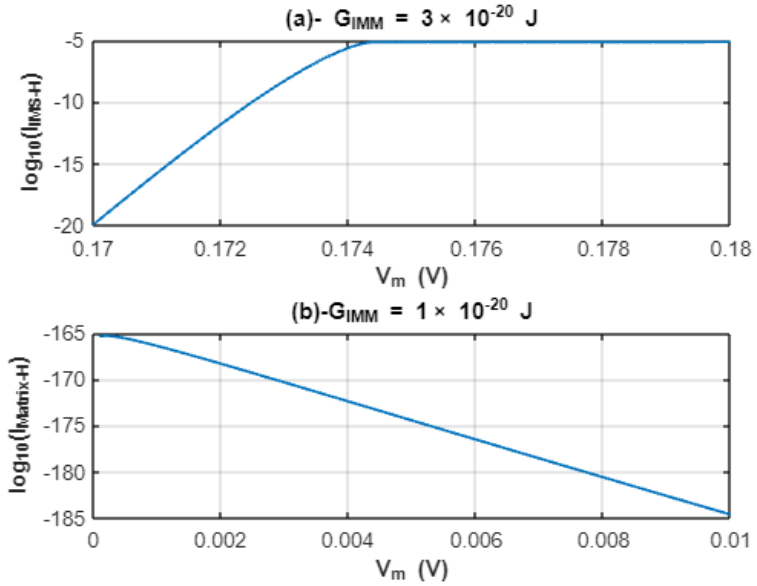

Figure 28. The figure represents the relationship between the potential of IMM and the logarithm of the tunneling leak current through IMM for IMS and matrix protons as represented in (a) and (b), respectively.

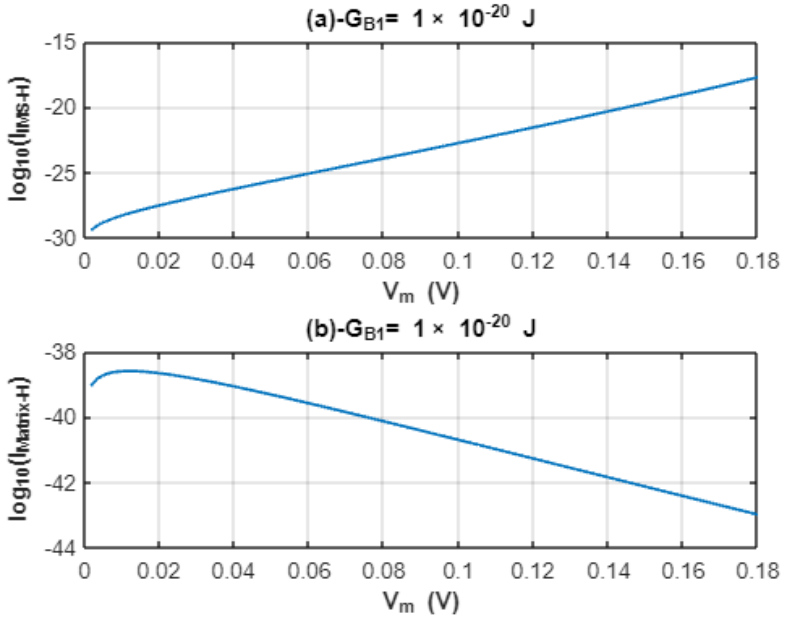

Figure 29. The figure represents the relationship between the potential of IMM and the logarithm of the tunneling leak current through B1 barrier for IMS and matrix protons as represented in (a) and (b), respectively.

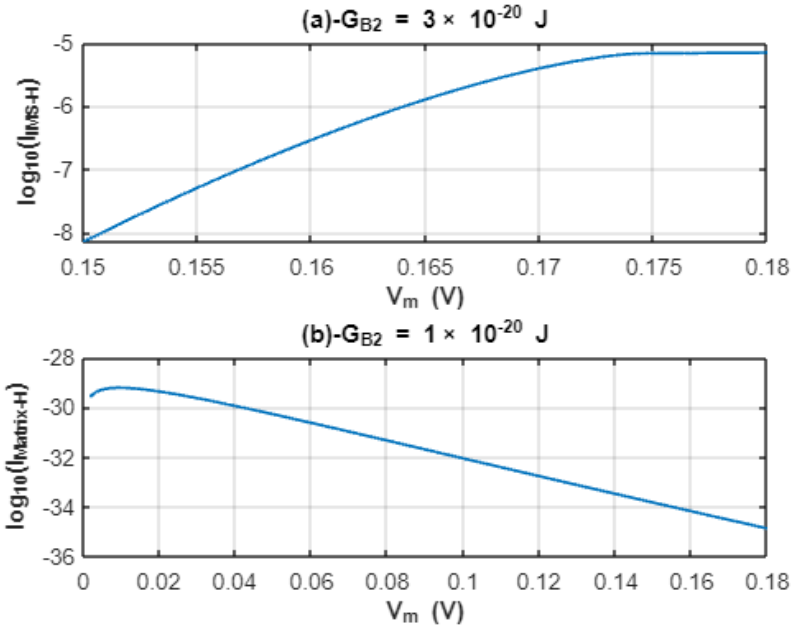

Figure 30. The figure represents the relationship between the potential of IMM and the logarithm of the tunneling leak current through B2 barrier for IMS and matrix protons as represented in (a) and (b), respectively.

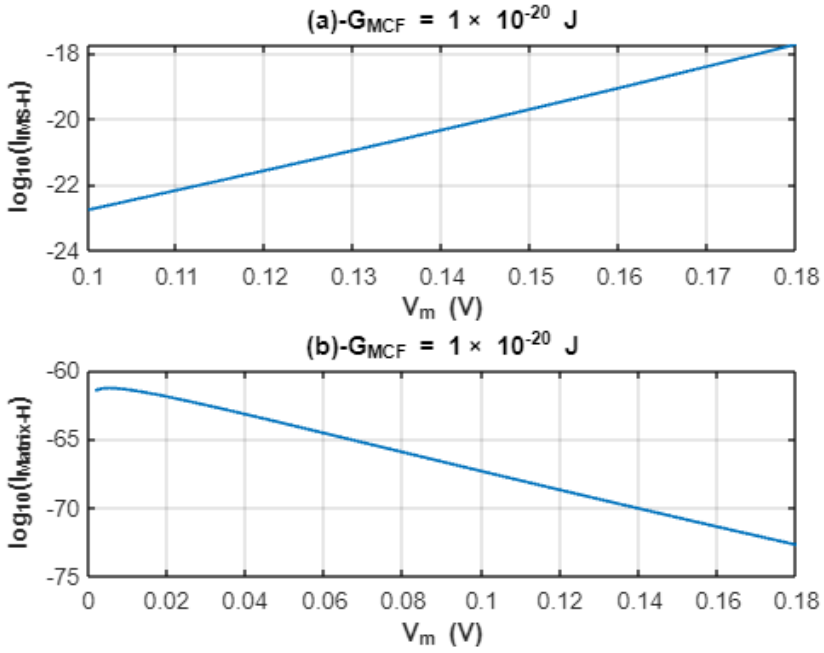

Figure 31. The figure represents the relationship between the potential of IMM and the logarithm of the tunneling leak current through B1 and B2 barriers for IMS and matrix protons as represented in (a) and (b), respectively.

4. Discussion

4.1. The quantum tunneling of protons through the inner mitochondrial membrane

The mitochondrion is a vital cellular organelle for ATP production, which provides cells with energy for physiological functions. ATP production is made via the proton flow through the ATPase protein in the inner mitochondrial membrane. The flow of protons is mainly dependent on the membrane potential of the inner mitochondrial membrane, which is positive at the side of intermembrane space IMS with respect to the matrix. However, not all the protons flowing through the inner mitochondrial membrane are utilized to generate ATP. Some of these protons leak through the inner membrane and the uncoupling proteins to control the production rate of ATP and ROS [8]. If there were a loss of the proton leak, excess production of ROS would result and in turn, would harm the cells. On the other hand, an increase in the proton leak would result in a decrease in ATP production which can also harm the cells. The reduction in ATP production by the proton leak current is mediated by two mechanisms: 1) Dissipating a proportion of the proton flow without being used in phosphorylation 'uncoupled oxidative phosphorylation [8]. 2) Membrane depolarization, which decreases the main force required for protons to flow through the ATPase [9–11].

Quantum biology is an interdisciplinary field that studies the intersection between quantum mechanics and biology. It aims to investigate the quantum effects on the biological processes [13,14]. One of the major particles that has been the focus of quantum biology is the proton, which has been studied in the context of DNA mutation [17,18] and proton tunneling in enzymes [19]. Thus, in our present work, we investigate the quantum behavior of protons and the role of their quantum tunneling in the proton leak and its influence on the electrical potential of the inner mitochondrial membrane. Up to the authors' knowledge, the present work is the first paper that explores the role of quantum tunneling of protons in mitochondria particularly its role in the proton leak. The proton leak current is mediated through the inner mitochondrial membrane itself and the uncoupling proteins. Hence, we apply the model of proton quantum tunneling on these two molecular structures. The proton tunneling implies that the proton has a non-zero probability of going through an energy barrier whose energy is higher than the energy of the proton. In the context of the proton passage through the inner mitochondrial membrane, the protons have the potential capacity to pass via quantum tunneling through the membrane itself and the closed uncoupling proteins. The probability of quantum tunneling of protons depends on the energy barrier height, its width, and the membrane potential of the inner mitochondrial membrane. As the energy barrier height and its width decrease, the tunneling probability increases and vice versa. In addition, the changes in membrane potential can affect the barrier height and/or the kinetic energy of protons, hence it is an important factor that modulates the tunneling probability.

The probability of quantum tunneling of protons from the intermembrane space is higher than that for the protons in the matrix. This discrepancy is due to the differences in the height of barriers they pass through and their kinetic energy due to the effect of the electric field of IMM. The protons in the intermembrane space acquire higher kinetic energy because they go through the membrane potential along with the same direction of the electric field, which is from the intermembrane space to the matrix. In addition, since the IMS protons flow along the same direction of the electric field, it will decrease the barrier height of IMM and MCF. On the other hand, the membrane potential imposes an energy barrier and decreases the kinetic energy of matrix protons, therefore, they have a lower tunneling probability. As a result, it is expected that there will be a net flow of protons to the matrix,

which may uncouple the oxidation from the phosphorylation and depolarize the electrical potential of the inner mitochondrial membrane IMM. The quantum tunneling of protons can occur through the inner mitochondrial membrane itself or the MCF proteins. However, differences exist between them due to the differences in the molecular structure and thus in the characteristics of the energy barrier. The whole inner mitochondrial membrane with a thickness of 7×10^{-9} m represents an energy barrier that impends the passage of protons. On the other hand, the MCF proteins possess two energy barriers consisting of salt bridges on the matrix and intermembrane space sides. In the present study, we assume an approximate value of 1×10^{-9} m for the length of each network of salt bridges and we propose five models of the protons quantum tunneling through the MCF proteins as in Figures 3 and 17.

Even though the width of the energy barrier for the inner mitochondrial membrane is larger than that for salt bridges barriers B1 and B2, the tunneling through the inner membrane can be significant due to the larger membrane potential involved in lowering the barrier height for protons across the length of inner membrane especially as the barrier height decreases. If Figures (5)−(8) are compared, it is clear that the tunneling probability of protons increases as the barrier height decreases especially in the case of the tunneling through the B2 barrier only, which showed greater sensitivity to the drop in the barrier height compared to the other barriers. Furthermore, it is clear from Figures (5)−(8) that as the electrical potential of IMM increases, the tunneling probability of IMS protons increases, while the tunneling probability of matrix protons decreases as the electrical potential increases. As a consequence of the quantum tunneling of protons, a quantum tunneling current of protons and a quantum conductance are expected to occur. Based on the differences between the several barriers in terms of tunneling probability, the B2 barrier showed the highest tendency for larger quantum conductance values at larger values of barrier height if it is compared with the other barriers using Figures 9−16. However, all barriers including IMM show significant values of quantum conductance as the barrier height decreases.

4.2. The effect of quantum tunneling leak of protons on the membrane potential of IMM

The present work aims to investigate the impact of the quantum tunneling leak of protons on the electrical potential of IMM, which is a main driving force of ATP synthesis. We adopted two approaches regarding the generation of the electrical potential of IMM. These approaches include: 1) The proton flow-based approach and 2) The approach of electrostatic density of protons. The approach of protons flow states that the flux of protons across the IMM is responsible for membrane potential generation. This approach is similar to the mechanism of membrane potential generation in neurons and cardiac cells, which is calculated using the Goldman-Hodgkin-Katz (GHK) equation. This means that the concentration and the conductance of protons determine the value of membrane potential. On the other hand, the approach of the electrostatic density of protons states that the accumulation of charges of protons at the IMS and matrix sides creates the potential difference across the membrane without the involvement of protons flow. Hence, the membrane conductance of protons in this approach has no role in membrane potential.

According to Figure 18, the proton flow-based approach predicts that the net quantum tunneling flux to the matrix through IMM can depolarize its electrical potential below 180 mV. However, this does not happen until the barrier height of IMM decreases to around 3×10^{-20} J or less. Thus, protons tunneling through barriers whose heights are larger than 3×10^{-20} J cannot affect the electrical membrane potential of IMM. Furthermore, in this case, the process of depolarization does not switch the original polarization, which means that the electrical potential will be positive at the IMS side

relative to the matrix side. Hence, as the barrier height of IMM decreases, the membrane potential decreases below 180 mV without switching the IMM electrical polarity. On the other hand, the approach of electrostatic density of protons predicts different patterns of change in the electrical potential. According to Figure 19, it is clear that there is a switch in the electrical polarity of IMM in which the IMS side becomes negative relative to the matrix side. Moreover, the switch in the polarity is observed across all values of the barrier height. Additionally, as the barrier height of IMM decreases, the electrical potential becomes less negative and more near zero but never goes above zero. Switching the electrical polarity according to the electrostatic approach is not compatible with the bioenergetics of mitochondria because in this case, the proton flow across ATP–synthase will be compromised.

Interestingly, the influence of proton tunneling through MCF proteins on the electrical potential of IMM has different characteristics that distinguish them from the influence of proton tunneling through the IMM itself. Based on Figure 20 which represents the influence of the barrier height on the membrane potential according to the first model, it is clear that no real mathematical solution for membrane potential exists when the values of the barrier height are within the range $(0.7-3)\times10^{-20}$ J because the two barriers B1 and B2 differ significantly in terms of utilizing the membrane potential for the kinetic energy of protons. This significant difference is attributed to the locations of B1 and B2. The B1 barrier exploits a smaller proportion of membrane potential, while the B2 barrier exploits a larger proportion. Hence, no solution is expected to be found when both barriers are closed within the range mentioned before. This means that there is no physical or biological meaning for both barriers to be closed within these range values of the barrier height. However, when the value of barrier height decreases below 0.7×10^{-20} J, the presence of both B1 and B2 has a physical and biological meaning. This meaning is the ability of proton tunneling to depolarize the IMM within a range of small values of membrane potential from around 30 mV to zero. On the other hand, when the approach of electrostatic density is adopted, the proton tunneling through the closed B1 and B2 results in the switch in the electrical polarity of IMM across all values of the barrier height, which is bio-energetically incompatible. In addition, as the barrier height decreases, the membrane potential becomes less negative with small changes in the potential relative to the changes in the barrier height (Figure 21).

According to Figures 22-25, in the second model in which proton tunneling occurs through the B1 barrier only, the proton flow-based approach predicts that the net proton tunneling to the matrix can depolarize the electrical potential of IMM below 180 mV when the barrier height decreases to less than 1.5×10^{-20} J. However, the proton tunneling does not affect the membrane potential if the barrier height is higher than 1.5×10^{-20} J. In addition to that, when the barrier height decreases to around 0.5×10^{-20} J or less, the proton tunneling will switch the electrical polarity of IMM until reaching −0.1 V, which can compromise the ATP production as in conditions of neurodegenerative diseases. On the other hand, based on the electrostatic density approach, the proton tunneling will switch the electrical polarity of IMM across all values of barrier height. However, proton tunneling will make the membrane potential less negative as the barrier height decreases within the range of values less than 2×10^{-20} J, whereas the membrane potential becomes more negative as the barrier height decreases within the range of values larger than 2×10^{-20} J. In the third model in which the proton tunneling occurs through the B2 barrier, proton tunneling can depolarize the membrane potential at barrier height values around 5×10^{-20} J or less and as the barrier height decreases, the electrical potential becomes more depolarized until reaching zero V without a switch in the electrical polarity of IMM. On the other hand, the electrostatic approach predicts that proton tunneling will switch the electrical polarity of IMM across all values of the barrier height and the membrane potential becomes less negative as the barrier height decreases. In the fourth model in which IMS protons tunnel through the B1 barrier and the matrix

protons tunnel through the B2 barrier, the proton tunneling can depolarize the membrane potential below 180 mV when the barrier height decreases below 1.5×10^{-20} J with a minimal switch in the electrical polarity of IMM below zero V at lower values of barrier height. According to the electrostatic approach, proton tunneling switches the electrical polarity of IMM and the membrane potential becomes less negative as the barrier height decreases. In the fifth model in which the IMS protons tunnel through the B2 barrier and the matrix protons tunnel through the B1 barrier, they can depolarize the membrane potential below 180 mV at a barrier height value around 5×10^{-20} J or less. In addition, as the barrier height decreases, the membrane potential becomes more depolarized until a minimal switch in the electrical polarity of the IMM occurs at lower values of barrier height. The electrostatic approach predicts a switch in the electrical polarity of IMM under the influence of protons quantum tunneling that shifts the membrane potential to less negative values as the barrier height decreases and vice versa.

Protons also can be transported through the IMM and MCF proteins classically. This implies that protons must obtain energy equal to or higher than the barrier height, otherwise no transport can take place. According to classical electrochemistry, the classical conductance values of protons at the matrix and IMS sides are the same, unlike the quantum tunneling model which shows a significant difference between protons on both sides in terms of tunneling probability and quantum conductance as explained before. Based on the proton flow-based approach, the opening of MCF proteins allows the classical transport of protons down their concentration gradient from the IMS side to the matrix side. This classical transport can depolarize the electrical potential of IMM without a switch in its electrical polarity as presented in Figures 26 and 27. However, if the electrostatic approach is considered, the classical transport of protons will switch the polarity of IMM towards the equilibrium potential of protons or the Nernst potential of protons, which is around −0.05 V.

Even though both the quantum and classical proton leak can depolarize the electrical potential of IMM, the major difference between them is that quantum tunneling-induced depolarization is more energetically favorable since protons do not need to get energy equal to or higher than the barrier height. Furthermore, no significant difference between the two types of transport in terms of the values of barrier height at which the leak becomes significant and depolarizes the membrane potential. Generally, according to our results, the depolarization induced by proton leak begins once the barrier height drops to $(2-1.5)\times10^{-20}$ J or less for both types of leak. However, proton tunneling through certain barriers can depolarize the potential at higher values as in the depolarization induced at 3×10^{-20} J in the case of proton tunneling through IMM and in the depolarization induced at 5×10^{-20} J in the case of IMS proton tunneling through B2 barrier only as in the third and fifth model of MCF proteins. As a result, it seems that the proton tunneling has an energetic advantage over the classical transport. In addition, the depolarization induced by quantum tunneling is much less dependent on the number of uncoupling proteins if it is compared with the classical transport. This observation can be noticed if the graphs of depolarization, in the results section, are compared for both types of transport. These graphs show that there is lesser variation in the values of membrane potential as the density of uncoupling proteins changes. Therefore, the quantum behavior of protons is equally important or even more important than the classical behavior, which deserves to be focused on in future research. In other words, when the barrier height of the salt bridges decreases, both the quantum and classical leaks increase, but it is more likely that the quantum leak might contribute more significantly due to the lower energetic requirement for ions to pass and the decreased dependence on the density of uncoupling proteins. Additionally, the electrical potential of the IMM modulates the proton leak current mediated by quantum tunneling. If the membrane potential increases, the tunneling leak current and quantum conductance are increased to decrease the electrical potential and vice versa. Moreover, the major determinant of the classical and

quantum leak is whether the barrier height is lower or higher than the energy of protons. If the barrier height is lower than the energy of protons, then classical transport is expected to occur, while if the barrier height is higher than the energy of protons, then quantum transport is expected to occur.

We focus on the tunneling leak current mediated via uncoupling proteins and the IMM. However, other promising molecular targets are candidates to apply the principles of quantum mechanics on. Other possible targets include ATPase which can run in both directions and other ion channels within the IMM. According to the present calculations, the quantum tunneling process might be important in increasing the efficiency of ATP production by the ATP synthase because quantum tunneling implies that ions can permeate through barriers by energy that is lower than the energy of the barrier. Hence, future works and investigations should focus on these molecular structures to determine the significance of the quantum tunneling of protons in the efficiency of energy production.

4.3. The role of quantum tunneling to the proton leak current

The occurrence of proton leak can be understood if the mitochondrial membrane is viewed as a flux capacitor in which the charges are stored to generate an electric field across the membrane while ions can flow in both directions and can change the strength of the electric field and thus the electrical voltage [35]. Based on Figures (28)−(31), several conclusions can be surmised regarding the tunneling leak current. The relationship between the tunneling leak current and the membrane potential is non-linear or non-ohmic. The tunneling current of IMS protons increases exponentially as the membrane potential increases, while the tunneling current of matrix protons decreases exponentially as the membrane potential increases. In addition, the tunneling leak current of IMS protons is much larger than matrix protons, which leads to the leak tunneling current being in the direction from IMS to the matrix of mitochondria. Furthermore, the tunneling leak current has a wide spectrum of values that are influenced by type of the barrier, the barrier height, and the membrane potential. It increases as the barrier height decreases but this varies according to the type of barrier imposed in front of protons. The inner mitochondrial membrane IMM and B2 barriers permeate significant leak current at higher values of barrier height i.e. at $G = 3\times10^{-20}$ J, while the B1 and MCF barriers (B1 and B2 are closed) permeate the same significant current or less at lower values of barrier height i.e. at $G = 1\times10^{-20}$ J. It contributes significantly to the proton leak current because if the tunneling current values in Figures (28)−(31) are compared with the classical leak current $I = CV = 10^{-17}\times0.18 = 1.8\times10^{-18}$ A, the tunneling current shows comparable or even higher values than the classical ones. Interestingly, it seems that proton tunneling contributes to the dissipation process occurring in mitochondria because tunneling exhibits significant values of leak current through the IMM and uncoupling proteins. This dissipation is critical in controlling ROS production, generates heat, and is involved in cell signaling. This suggests that dissipation mediated via tunneling leak current has an anti-inflammatory effect [16]. Moreover, uncoupling is not limited to the backflow of protons but may include other ions including calcium and potassium ions which may contribute to the dissipation process. Hence, the quantum tunneling of these ions warrants further investigations to explore their influence on the electrical potential of the IMM. Furthermore, cells can capture energy through the gradients of ions across other membranes and are not limited to the mitochondrial membrane. Therefore, this indicates that quantum tunneling might play a crucial role in the energy extraction in other vital cellular processes including facilitated diffusion mediated by carrier proteins. Quantum tunneling might be a survival and adaptive mode of transport that conserves energy because the mathematical results indicate that tunneling consumes less energy compared to the classical one to accomplish the same metabolic tasks.

A recent interesting study showed that using voltage dyes of lipophilic cations the changes in the electrical potential of the IMM can be visualized by a high resolution under different metabolic states including the effect of inducing the leak proton current [36]. Hence, this method of investigation can be utilized to visualize the influence of the tunneling current of protons on the electrical potential and perhaps to infer a unique pattern of voltage dynamics that can be distinctive from the pattern induced by the classical leak current. This may provide experimental evidence on the theoretical results obtained in Figures 18−25 and Figure 26, which delineate different patterns of changes in the voltage of IMM.

4.4. Implications to aging, inflammation and diseases

The uncoupling proteins can modulate the electrical potential of the inner mitochondrial membrane IMM and thus can affect the production of ROS that contribute to oxidative stress and the production of ATP which is a major energy source for normal neurological functioning [37−39]. In healthy cells, the mitochondrion couples between the ATP and ROS production in such a way that the increase in ATP production is associated with an increase in ROS production and vice versa. Hence, the balance between ATP and ROS production is fine-tuned, which ensures providing adequate energy for cellular functions while minimizing the collateral damage made by ROS. The aging process involves a mitochondrial dysfunction which results in a decline in ATP production which puts the cells at the risk of apoptosis. Consequently, apoptosis triggers an inflammatory response which leads to an increase in the levels of ROS. Aging, inflammation, and the pathophysiological processes of several diseases affect the integrity of membranes, their curvature, and lipid composition [40]. All these changes may alter the shearing and tension forces on the pore-forming proteins such as uncoupling proteins. This may lead to a decrease in the barrier height of the closed gate and thus an increase in the tunneling probability and the tunneling leak of protons [40,41]. In addition, if the process of uncoupling leads to a significant reduction in the membrane potential of the IMM beyond the redox-optimized ROS balances, a state of low-energy oxidative phase ensues due to the decreased rate of ROS scavenging [42]. As a result, elevated levels of ROS cause oxidative damage to DNA, proteins, lipids, and other components of the cell. These harmful effects predispose cells to inflammation, carcinogenesis, and cell death.

Under pathological conditions including neurodegenerative diseases and ischemic heart diseases, there will be a decoupling between the production of ATP and ROS, which means that the decrease in ATP level is associated with an increase in ROS production [43]. Moreover, these pathological conditions can disrupt the functions of mitochondria, especially within the inner mitochondrial membrane as part of the aging process [37−46]. The aging-related disruption affects the integrity of the IMM and its proteins including the MCF proteins [37−47]. This leads to an increase in their permeability possibly due to the reduction in the barrier height values from a bioenergetics perspective [37–47]. As we explained earlier in the study, the decrease in the barrier height of IMM and the salt-bridge networks will enhance the proton leak flow either via quantum tunneling or classical transport that will depolarize the membrane potential. Within the normal physiological functioning of mitochondria, mild depolarization can be protective by decreasing the level of ROS associated with lowering ATP production due to the proton leak itself and membrane depolarization. However, when the drop in the barrier height becomes beyond the physiological limits, the membrane depolarization will be overwhelming so the decrease in ATP production will be intolerable to mitochondria and cells. Eventually, an increase in ROS production oxidative stress, and cell death will ensue [37−46].

Therefore, targeting the proton leak current may offer promising therapeutic drugs to manage challenging neurological diseases. In addition, taking into consideration the quantum behavior of protons in this context will provide effective pharmacological interventions because the quantum tunneling behavior is influential and more energetically favorable making its influence on the progression of these diseases remarkable. Accordingly, if oxidative stress is our major concern, then augmenting the quantum tunneling of protons will alleviate it [48], while if our major concern is the low ATP production, then inhibiting the quantum tunneling of protons will increase ATP production.

5. Conclusions

We speculated that tunneling leak flow of protons might have an important role in the physiological regulation of the leak current and modulation of the electrical potential of the inner mitochondrial membrane IMM. Moreover, the quantum-tunneling leak of protons might be more energetically favorable giving it more advantage over the classical leak of protons to dominate. In this theoretical framework, we assume that tunneling-induced membrane depolarization may have deleterious effects on cells because large IMM depolarization can deplete the ATP level, which increases the level of oxidative stress due to the higher rate of ROS production. Eventually, neuronal cell death occurs as observed in many neurodegenerative diseases. More importantly, our mathematical results suggest that quantum tunneling of protons can occur in a strong electric field as the same found across the IMM. Interestingly, the electric field may augment the probability of quantum tunneling and conserve the energy required for metabolic and cellular functions.

The key message of the present paper is to shed light on the importance of considering the quantum wave behavior of protons in the functioning of mitochondria and motivate researchers to conduct theoretical and experimental works to explore additional quantum aspects in the function of mitochondria and the cell as a whole.

Use of AI tools declaration

The authors declare they have not used Artificial Intelligence (AI) tools in the creation of this article.

Data Availability Statement

The data are available upon a reasonable request from the corresponding author.

Conflicts of interest

The authors declare no conflict of interest.

Author contributions

Conceptualization, A.B.Q and M.A; methodology, A.B.Q; software, A.B.Q.; validation, A.B.Q, M.A., M.E.,A.R.Q., Q.A., R.S., L.K., M.M., A.A., H.M., H.A., B.A., R.O., M.A., S.I., F.T., A.D., B.D.,A.H., M.A., S.A., S.B.H., and R.M.; formal analysis, A.B.Q.; investigation, A.B.Q..; resources,

A.B.Q, M.A., M.E.,A.R.Q., Q.A., R.S., L.K., M.M., A.A., H.M., H.A., B.A., R.O., M.A., S.I., F.T., A.D., B.D.,A.H., M.A.,S.A., S.B.H., and R.M.; data curation, A.B.Q, M.A., M.E.,A.R.Q., Q.A., R.S., L.K., M.M., A.A., H.M., H.A., B.A., R.O., M.A., S.I., F.T., A.D., B.D.,A.H., M.A., S.A., S.B.H., and R.M.; writing—original draft preparation, A.B.Q.; writing—review and editing, A.B.Q, M.A., M.E.,A.R.Q., Q.A., R.S., L.K., M.M., A.A., H.M., H.A., B.A., R.O., M.A., S.I., F.T., A.D., B.D.,A.H., M.A., S.A., S.B.H., and R.M.; visualization, A.B.Q.; supervision, M.A. and R.M..; project administration, M.A. and R.M. All authors have read and agreed to the published version of the manuscript.

References

1. Picard M, Taivassalo T, Gouspillou G, et al. (2011) Mitochondria: isolation, structure and function. *J Physiol* 589: 4413–4421. https://doi.org/10.1113/jphysiol.2011.212712
2. Duchen MR (2004) Roles of mitochondria in health and disease. *Diabetes* 1: S96−102. https://doi.org/10.2337/diabetes.53.2007.S96
3. Ardalan A, Smith MD, Jelokhani-Niaraki M (2022) Uncoupling proteins and regulated proton leak in mitochondria. *Int J Mol Sci* 23: 1528. https://doi.org/10.3390/ijms23031528
4. Nesci S (2023) Proton leak through the UCPs and ANT carriers and beyond: a breath for the electron transport chain. *Biochimie* 214: 77−85. https://doi.org/10.1016/j.biochi.2023.06.008
5. Jastroch M, Divakaruni AS, Mookerjee S, et al. (2010) Mitochondrial proton and electron leaks. *Essays Biochem* 47:53−67. https://doi.org/10.1042/bse0470053
6. Bertholet AM, Kirichok Y (2022) Mitochondrial H^+ leak and thermogenesis *Annu Rev Physiol* 84: 381−407. https://doi.org/10.1146/annurev-physiol-021119-034405
7. Nicholls DG (1997) The non-Ohmic proton leak—25 years on. *Biosci Rep* 17: 251−257. https://doi.org/10.1023/A:1027376426860
8. Rupprecht A, Sokolenko EA, Beck V, et al. (2010) Role of the transmembrane potential in the membrane proton leak. *Biophys J* 98: 1503−1511. https://doi.org/10.1016/j.bpj.2009.12.4301
9. Kenwood BM, Weaver JL, Bajwa A, et al. (2014) Identification of a novel mitochondrial uncoupler that does not depolarize the plasma membrane. *Mol Metab* 3: 114−123. https://doi.org/10.1016/j.molmet.2013.11.005
10. Sack MN (2006) Mitochondrial depolarization and the role of uncoupling proteins in ischemia tolerance. *Cardiovasc Res* 72: 210−219. https://doi.org/10.1016/j.cardiores.2006.07.010
11. Padmaraj D, Pande R, Miller Jr JH, et al. (2014). Mitochondrial membrane studies using impedance spectroscopy with parallel pH monitoring. *PLoS One* 9: e101793. https://doi.org/10.1371/journal.pone.0101793
12. Serway RA, Kirkpatrick LD (2005) Physics for Scientists and Engineers with Modern Physics James Madison University. https://doi.org/10.1119/1.2342517
13. Calvillo L, Redaelli V, Ludwig N, et al. (2022) Quantum biology research meets pathophysiology and therapeutic mechanisms: a biomedical perspective. *Quantum Rep* 4: 148−712. https://doi.org/10.3390/quantum4020011
14. Kim Y, Bertagna F, D'souza EM, et al. (2021) Quantum biology: an update and perspective. *Quantum Rep* 3: 80−126. https://doi.org/10.3390/quantum3010006
15. Bennett Jr JP, Onyango IG (2021) Energy, entropy and quantum tunneling of protons and electrons in brain mitochondria: relation to mitochondrial impairment in aging-related human brain diseases and therapeutic measures. *Biomedicines* 9: 225. https://doi.org/10.3390/biomedicines9020225

16. Nunn AV, Guy GW, Bell JD (2022) Thermodynamics and inflammation: insights into quantum biology and ageing. *Quantum Rep* 4: 47−74. https://doi.org/10.3390/quantum4010005
17. Slocombe L, Sacchi M, Al-Khalili J (2022) An open quantum systems approach to proton tunnelling in DNA. *Commun Phys* 5: 109. https://doi.org/10.1038/s42005-022-00881-8
18. Çelebi G, Özçelik E, Vardar E, et al. (2021) Time delay during the proton tunneling in the base pairs of the DNA double helix. *Prog Biophys Mol Biol* 167: 96−103. https://doi.org/10.1016/j.pbiomolbio.2021.06.001
19. Layfield JP, Hammes-Schiffer S (2014) Hydrogen tunneling in enzymes and biomimetic models. *Chem Rev* 114: 3466−3494. https://doi.org/10.1021/cr400400p
20. Xin H, Sim WJ, Namgung B, et al. (2019) Quantum biological tunnel junction for electron transfer imaging in live cells. *Nat Commun* 10: 3245. https://doi.org/10.1038/s41467-019-11212-x
21. Hayashi T, Stuchebrukhov AA (2010) Electron tunneling in respiratory complex I. *Proc Natl Acad Sci USA* 107: 19157−19162. https://doi.org/10.1073/pnas.1009181107
22. Hagras MA, Hayashi T, Stuchebrukhov AA (2015) Quantum calculations of electron tunneling in respiratory complex III. *J Phys Chem B* 119: 14637−14651. https://doi.org/10.1021/acs.jpcb.5b09424
23. Gray HB, Winkler JR (2003) Electron tunneling through proteins. *Q Rev Biophys* 36: 341−372. https://doi.org/10.1017/S0033583503003913
24. Qaswal AB (2019) Quantum tunneling of ions through the closed voltage-gated channels of the biological membrane: A mathematical model and implications. *Quantum Rep* 1: 219−225. https://doi.org/10.3390/quantum1020019
25. Qaswal AB, Ababneh O, Khreesha L, et al. (2021) Mathematical modeling of ion quantum tunneling reveals novel properties of voltage-gated channels and quantum aspects of their pathophysiology in excitability-related disorders. *Pathophysiology* 28: 116−154. https://doi.org/10.3390/pathophysiology28010010
26. Vorobyov I, Olson TE, Kim JH, et al. (2014) Ion-induced defect permeation of lipid membranes. *Biophys. J* 106: 586−597. https://doi.org/10.1016/j.bpj.2013.12.027
27. Aryal P, Sansom MS, Tucker SJ (2015) Hydrophobic gating in ion channels. *J Mol Biol* 427: 121−130. https://doi.org/10.1016/j.jmb.2014.07.030
28. Khavrutskii IV, Gorfe AA, Lu B (2009) Free energy for the permeation of Na^+ and Cl^- ions and their ion-pair through a zwitterionicdimyristoyl phosphatidylcholine lipid bilayer by umbrella integration with harmonic fourier beads. *J Am Chem Soc* 131: 1706−1716. https://doi.org/10.1021/ja8081704
29. Klesse G, Tucker SJ, Sansom MS (2020) Electric field induced wetting of a hydrophobic gate in a model nanopore based on the 5-HT3 receptor channel. *ACS Nano* 14: 10480−10491. https://doi.org/10.1021/acsnano.0c04387
30. Miyazaki T (2004) *Atom Tunneling Phenomena in Physics, Chemistry and Biology*, Berlin: Springer Science & Business Media. https://doi.org/10.1007/978-3-662-05900-5
31. Bertil H, Bertil H (2001) *Ion Channels of Excitable Membranes*, Sunderland: Sinauer Associates. https://doi.org/10.1016/0014-5793(92)81020-m
32. Lee JW (2019) Electrostatically localized proton bioenergetics: better understanding membrane potential. *Heliyon* 5: e01961. https://doi.org/10.1016/j.heliyon.2019.e01961
33. Silverstein TP (2022) A critique of the capacitor-based "transmembrane electrostatically localized proton" hypothesis. *J Bioenerg Biomembr* 54: 59−65. https://doi.org/10.1007/s10863-022-09931-w

34. Qaswal AB (2020) Quantum electrochemical equilibrium: quantum version of the Goldman–Hodgkin–Katz equation. *Quantum Rep* 2: 266−277. https://doi.org/10.3390/quantum2020017
35. Lee JW (2020) Protonic capacitor: elucidating the biological significance of mitochondrial cristae formation. *Sci Rep* 10: 10304. https://doi.org/10.1038/s41598-020-66203-6
36. Lee C, Wallace DC, Burke PJ (2023) Super-resolution imaging of voltages in the interior of individual, vital mitochondria. *Acs Nano* 18: 1345−1356. https://doi.org/10.1021/acsnano.3c02768
37. Nicholls D (2002) Mitochondrial bioenergetics, aging, and aging-related disease. *Sci Aging Knowl Environ* 2002: pe12. https://doi.org/10.1126/sageke.2002.31.pe12
38. Norat P, Soldozy S, Sokolowski JD et al. (2020) Mitochondrial dysfunction in neurological disorders: Exploring mitochondrial transplantation. *NPJ Regen Med* 5: 22. https://doi.org/10.1038/s41536-020-00107-x
39. Brookes PS, Land JM, Clark JB, et al. (1998) Peroxynitrite and brain mitochondria: evidence for increased proton leak. *J Neurochem* 70: 2195−2202. https://doi.org/10.1046/j.1471-4159.1998.70052195.x
40. Xie P, Zhang H, Qin Y, et al. (2023) Membrane proteins and membrane curvature: mutual interactions and a perspective on disease treatments. *Biomolecules* 13: 1772. https://doi.org/10.3390/biom13121772
41. Morris CE (2011). Voltage-gated channel mechanosensitivity: fact or friction?. *Front Physiol* 2: 25. https://doi.org/10.3389/fphys.2011.00025
42. Cortassa S, O'Rourke B, Aon MA (2014) Redox-optimized ROS balance and the relationship between mitochondrial respiration and ROS. *Biochim Biophys Acta* 1837: 287−295. https://doi.org/10.1016/j.bbabio.2013.11.007
43. vanHameren G, Campbell G, Deck M, et al. (2019) In vivo real-time dynamics of ATP and ROS production in axonal mitochondria show decoupling in mouse models of peripheral neuropathies. *Acta Neuropathol Commun* 7: 86. https://doi.org/10.1186/s40478-019-0740-4
44. Berry BJ, Kaeberlein M (2021) An energetics perspective on geroscience: mitochondrial protonmotive force and aging. *Geroscience* 43: 1591−1604. https://doi.org/10.1007/s11357-021-00365-7
45. Berry BJ, Mjelde E, Carreno F, et al. (2023) Preservation of mitochondrial membrane potential is necessary for lifespan extension from dietary restriction. *GeroScience* 45: 1573−1581. https://doi.org/10.1007/s11357-023-00766-w
46. Sutherland TC, Sefiani A, Horvat D, et al. (2021) Age-dependent decline in neuron growth potential and mitochondria functions in cortical neurons. *Cells* 10: 1625. https://doi.org/10.3390/cells10071625
47. Zhang H, Alder NN, Wang W, et al. (2020) Reduction of elevated proton leak rejuvenates mitochondria in the aged cardiomyocyte. *Elife* 9: e60827. https://doi.org/10.7554/eLife.60827
48. Barnstable CJ, Zhang M, Tombran-Tink J (2022) Uncoupling proteins as therapeutic targets for neurodegenerative diseases. *Int J Mol Sci* 23: 5672. https://doi.org/10.3390/ijms23105672

AIMS Press